AIAA Guidance, Navigation and Control Conference and Exhibit
18 - 21 August 2008, Honolulu, Hawaii

AIAA 2008-6472

Attitude and Phase Synchronization of Formation Flying Spacecraft: Lagrangian Approach

Soon-Jo Chung*

Iowa State University, IA 50011, USA

Umair Ahsun,† and Jean-Jacques E. Slotine‡

Massachusetts Institute of Technology, MA 02139, USA

This article presents a unified synchronization framework with application to precision formation flying spacecraft. Central to the proposed innovation, in applying synchronization to both translational and rotational dynamics in the Lagrangian form, is the use of the distributed stability and performance analysis tool, called contraction analysis that yields exact nonlinear stability proofs. The proposed decentralized tracking control law synchronizes the attitude of an arbitrary number of spacecraft into a common time-varying trajectory with global exponential convergence. Moreover, a decentralized translational tracking control law based on phase synchronization is presented, thus enabling coupled translational and rotational maneuvers. While the translational dynamics can be adequately controlled by linear control laws, the proposed method permits highly nonlinear systems with nonlinearly coupled inertia matrices such as the attitude dynamics of spacecraft whose large and rapid slew maneuvers justify the nonlinear control approach. The proposed method integrates both the trajectory tracking and synchronization problems in a single control framework.

I. Introduction

Motivated by distributed computation and cooperation, abundant in both biological systems (e.g., fish swarms) and artificial machines (e.g., parallel computers), formation flying spacecraft has been a key research topic among many recent advancements.[1–4] Multiple apertures flying in precise formation are expected to provide unprecedented image resolution, both for astronomy and reconnaissance,[5] as well as unparalleled reconfigurability. However, many significant technical challenges must be overcome before formation flying interferometers can be realized. For instance, formation flight requires extensive technology development for precise attitude and position maintenance of multiple spacecraft.

The objective of this paper is to introduce a unified synchronization framework that can be directly applied to the position and attitude synchronization, and cooperative control of formation flight networks, comprised of either identical or heterogenous spacecraft. Synchronization is defined as a complete match of all configuration variables of each dynamical system. We also introduce phase synchronization where spacecraft follow an oscillatory trajectory with some phase difference between spacecraft. In particular, we show that we can synchronize the attitudes and positions of multiple spacecraft faster than they track the common position and attitude trajectories. The combined synchronization and tracking control law can achieve more efficient and robust performance through local interactions, especially in the presence of non-identical disturbances and uncertainties. Such local interactions are key to stellar formation flight interferometers that depend on precision control of relative spacecraft motions, indispensable for coherent interferometric beam combination.

This paper improve on our recent paper on the synchronization of multiple formation flying spacecraft[6] in multiple ways. First, we show that the linear translation dynamics with some nonlinear gravity terms

*Assistant Professor of Aerospace Engineering, AIAA Member, sjchung@alum.mit.edu.
†Research Affiliate, MIT Space Systems Laboratory, umair@alum.mit.edu.
‡Professor of Mechanical Engineering & Information Sciences, Professor of Brain & Cognitive Sciences, jjs@mit.edu.

can be written in a Lagrangian form. Such a formulation facilitates the use of the proposed control law that exploits the skew-symmetry of the dynamic terms. Second, in order to make the position synchronization more practical, we propose the phase synchronization of translational dynamics for a circular or spiral trajectory. The proof is more generalized to emphasize that there exist two different timescales (tracking dynamics, and synchronization dynamics).

A recent review paper[7,8] highlighted the three main areas for future research that have not been thoroughly addressed in the spacecraft formation flight literature: (1) rigorous stability conditions for cyclic and behavioral architectures, (2) reduced algorithmic information requirements, and (3) increased robustness/autonomy. While this paper does not provide complete solutions to these three challenges, we compare this paper with prior work in the aforementioned areas as follows:

1. Rigorous Stability Condition for Highly Nonlinear Time Varying Systems

Prior work on consensus and flocking problems using graphs, particularly popular in the robotics research community, tends to assume very simple dynamics such linear systems and single or double integrator dynamic models.[9–12] While such work can be generally applied to the synchronous spacecraft position control problem, which fares well with linear control, the proposed strategy in this paper primarily deals with complex dynamical networks consisting of highly nonlinear time-varying dynamics that are controlled to track a time-varying reference trajectory or leader. Examples of such a nonlinear system include the attitude dynamics of spacecraft for large and rapid slew maneuvers.

Some prior works on attitude synchronization rely on tracking a common reference (leader) spacecraft without interactions with local neighbors.[13,14] Local coupling control laws are suggested in Ref. 15, but individual spacecraft are synchronized to a constant state, thus not permitting an arbitrary reference trajectory. This is particularly true of consensus problems on graphs.[9] Compared with one recent work[16] that studied formation keeping and attitude alignment for multiple spacecraft with local couplings, the present paper also introduces a novel position consensus strategy using phase synchronization.

It should be noted that determining stability of nonlinear time-varying dynamic network systems is more involved and difficult.[17–19] Many mechanical systems exhibit nonlinear dynamics that cannot be captured by linearization. One might argue that most space systems are not required to follow demanding time-varying trajectories, thus validating linearization or linear coupling control laws. In particular, for the translational dynamics, a linear coupling control law can effectively stabilize the formation flying spacecraft. However, global exponential convergence of the attitude dynamics is achieved only through nonlinear control. For instance, there is increased interest in highly agile imaging spacecraft[20] that undergo wide and rapid slew angle changes. Moreover, in the context of nonlinear control theory, the asymptotic convergence of linear control, employed to stabilize nonlinear systems, may not be sufficient for demanding future mission requirements. In essence, ensuring exponential tracking stability for general nonlinear systems is made possible only through nonlinear control, and the benefit of exponential stability, in terms of improved tracking performance and robustness, is illustrated in this paper.

We introduce contraction analysis[21–24] as our main nonlinear stability tool for reducing the complexity and dimensionality associated with multi-agent systems, thereby deriving exact and global results with exponential convergence with respect to arbitrary time-varying inputs (see the Appendix for the further treatment of contraction theory).

2. Reduced Information Network

Another benefit of synchronization is its implication for model reduction. The exponential synchronization of multiple nonlinear dynamics allows us to reduce the dimensionality of the stability analysis of a large network. The model reduction aspect of synchronization, also introduced for spatially inter-connected systems in Ref. 2, is further generalized and strengthened in this article. This implies that once the network is proven to synchronize, we can regard a network as a single set of synchronized dynamics, which simplifies any additional stability analysis. As shall be seen later in the subsequent sections, this model reduction has to do with the fact that there are two time-scales associated with the coupled nonlinear dynamics.

In addition, the proposed control laws are of a decentralized form requiring only local velocity/position coupling feedback for global exponential convergence, thereby facilitating implementation in real systems. In contrast with some previous work using all-to-all coupling or depending only on tracking the same leader (reference) spacecraft without local interactions,[13,14] our proposed approach will not only reduce communication burdens, but also increase the overall performance of relative formation flight through local interactions.

3. Robustness Issues

The proposed method integrates both the trajectory tracking and synchronization problems toward a single control framework. Although an uncoupled trajectory control law, in the absence of external disturbances, would achieve synchronization to a common trajectory, the proposed control strategy can achieve more efficient and robust performance through synchronization using local interactions, especially if the external disturbances vary with each spacecraft.[17] In addition, the previous works do not discuss a property of robustness in detail. In contrast, we show that the proposed decentralized control law possesses a property of robustness to inter-spacecraft time-delays[4,6] and bounded disturbances. An adaptive version of the proposed control law is also presented to deal with parametric uncertainties of dynamic models.

Whereas our paper presents the unified decentralized control method for the Lagrangian dynamics of both rotational and translational motions of the spacecraft, with focus on minimizing the tracking and synchronization errors, the literature focused only on the relative translational motions is abundant. A disturbance accommodating control design process is presented in Ref. 25 for minimizing the total fuel consumption for the formation as well as maintaining the equal level of fuel consumption for each spacecraft. Ref. 26 presents a Hamiltonian approach to modelling relative spacecraft motion based on a derivation of canonical coordinates for the relative state-space dynamics, while another paper[27] introduces a new linear time-varying form of the equations of relative motions developed from Gauss's variational equations.

II. Lagrangian Formulation of Formation Flying Spacecraft

The proposed synchronization framework is devoted to the use of the Lagrangian formulation for its simplicity in dealing with complex systems involving multiple dynamics. We show herein that the rotational maneuvers of a rigid spacecraft can be written in this Lagrangian form, thereby permitting direct application of the proposed synchronization strategy[4,17] to the rotational dynamics of multiple spacecraft. Without loss of generality, the proposed control law can be applied to the position synchronization of formation flying spacecraft, or more generally to the coupled translational and attitude dynamics.

A. Lagrangian Formulation

The equations of motion for a spacecraft with multiple degrees-of-freedom ($\mathbf{q}_i \in \mathbb{R}^n$) can be derived by exploiting the Euler-Lagrange equations:

$$L_i(\mathbf{q}_i, \dot{\mathbf{q}}_i) = \frac{1}{2}\dot{\mathbf{q}}_i^T \mathbf{M}_i(\mathbf{q}_i)\dot{\mathbf{q}}_i - V_i(\mathbf{q}_i), \quad \frac{d}{dt}\frac{\partial L_i(\mathbf{q}_i, \dot{\mathbf{q}}_i)}{\partial \dot{\mathbf{q}}_i} - \frac{\partial L_i(\mathbf{q}_i, \dot{\mathbf{q}}_i)}{\partial \mathbf{q}_i} = \tau_i \tag{1}$$

where i, $(1 \leq i \leq p)$ denotes the index of spacecraft comprising a spacecraft formation flight network, and p is the total number of the individual elements. Equation (1) can be written as

$$\mathbf{M}_i(\mathbf{q}_i)\ddot{\mathbf{q}}_i + \mathbf{C}_i(\mathbf{q}_i, \dot{\mathbf{q}}_i)\dot{\mathbf{q}}_i + \mathbf{g}_i(\mathbf{q}_i) = \tau_i \tag{2}$$

where $\mathbf{g}_i(\mathbf{q}_i) = \frac{dV_i(\mathbf{q}_i)}{d\mathbf{q}_i}$, and, τ_i is a generalized force or torque acting on the i-th spacecraft.

It should be emphasized that, among many possible choices, the $\mathbf{C}$ matrix is defined as

$$c_{ij} = \frac{1}{2}\sum_{k=1}^{n}\frac{\partial M_{ij}}{\partial q_k}\dot{q}_k + \frac{1}{2}\sum_{k=1}^{n}\left(\frac{\partial M_{ik}}{\partial q_j} - \frac{\partial M_{jk}}{\partial q_i}\right)\dot{q}_k \tag{3}$$

Then, it is straightforward to show that $(\dot{\mathbf{M}}_i - 2\mathbf{C}_i)$ is skew-symmetric, resulting in

$$\mathbf{x}^T(\dot{\mathbf{M}}_i - 2\mathbf{C}_i)\mathbf{x} = 0, \quad 1 \leq i \leq p \tag{4}$$

for an arbitrary $\mathbf{x} \in \mathbb{R}^n$. This skew-symmetric property can be viewed as a matrix expression of energy conservation, which can also be explained in the context of the passivity formalism.[18] In the remainder of this paper, the property in (4) is extensively exploited for stability analysis and control synthesis using contraction theory.[4]

We assume that the spacecraft system in (2) is fully actuated. In other words, the number of control inputs is equal to the dimension of their configuration manifold (n).

B. Attitude Dynamics of Rigid Spacecraft

We present the Lagrangian formulation of the attitude dynamics introduced in Ref.[6] The following equations of motion are obtained with respect to the modified Rodrigues parameters[30,31] $\mathbf{q}_i$ for the i-th spacecraft $(1 \leq i \leq p)$

$$\mathbf{M}_i(\mathbf{q}_i)\ddot{\mathbf{q}}_i + \mathbf{C}_i(\mathbf{q}_i, \dot{\mathbf{q}}_i)\dot{\mathbf{q}}_i = \tau_i + \tau_{\mathbf{ext},i} \tag{5}$$

where the relationship between the corresponding quaternions $(\beta_1, \beta_2, \beta_3, \beta_4)$ and the modified Rodrigues parameters ($\mathbf{q} = (q_1, q_2, q_3)^T$) is given by

$$\beta_i = 2q_i/(1 + \mathbf{q}^T\mathbf{q}), \quad i = 1,2,3, \quad \beta_4 = (1 - \mathbf{q}^T\mathbf{q})/(1 + \mathbf{q}^T\mathbf{q}), \quad q_i = \beta_i/(1 + \beta_4), \quad i = 1,2,3 \tag{6}$$

Also,

$$\begin{aligned} \tau_i &= \mathbf{Z}^{-T}(\mathbf{q}_i)\mathbf{u}, \quad \tau_{\mathbf{ext},i} = \mathbf{Z}^{-T}(\mathbf{q}_i)\mathbf{d}_{\mathbf{ext},i} \\ \mathbf{M}_i(\mathbf{q}_i) &= \mathbf{Z}^{-T}(\mathbf{q}_i)\mathbf{J}_{\mathbf{s/c},i}\mathbf{Z}^{-1}(\mathbf{q}_i) \\ \mathbf{C}_i(\mathbf{q}_i, \dot{\mathbf{q}}_i) &= -\mathbf{Z}^{-T}\mathbf{J}_{\mathbf{s/c},i}\mathbf{Z}^{-1}\dot{\mathbf{Z}}\mathbf{Z}^{-1} - \mathbf{Z}^{-T}\mathbf{S}(\mathbf{J}_{\mathbf{s/c},i}\omega_i)\mathbf{Z}^{-1}. \end{aligned} \tag{7}$$

Notice that the index i has been added to $\mathbf{J}_{\mathbf{s/c},i}$ (hence, also to $\mathbf{M}_i$ and $\mathbf{C}_i$) to permit complex formation networks comprised of multiple heterogeneous spacecraft. Notice that all the terms in (5–7) are left-multiplied by $\mathbf{Z}^{-T}$. However, we should not cancel out the common term $\mathbf{Z}^{-T}$ of (5–7), which would result in having a non-symmetric $\mathbf{M}_i(\mathbf{q}_i)$. In essence, we established a Lagrangian formulation for the attitude dynamics of rigid spacecraft. This allows us to apply a wealth of nonlinear control laws to spacecraft dynamics, including the proposed control strategy in Ref. 17, that were originally developed for robot dynamics. As discussed in (4), the most important feature of (5) is to have a skew-symmetric $\dot{\mathbf{M}} - 2\mathbf{C}$ due to energy conservation. Indeed, we can verify that

$$\dot{\mathbf{M}}_i - 2\mathbf{C}_i = \frac{d\mathbf{Z}^{-T}}{dt}\mathbf{J}_{\mathbf{s/c},i}\mathbf{Z}^{-1} - \mathbf{Z}^{-T}\mathbf{J}_{\mathbf{s/c},i}\frac{d\mathbf{Z}^{-1}}{dt} + 2\mathbf{Z}^{-T}\mathbf{S}(\mathbf{J}_{\mathbf{s/c},i}\omega_i)\mathbf{Z}^{-1} \tag{8}$$

is skew-symmetric, which follows from that $\mathbf{S}(\mathbf{J}_{\mathbf{s/c},i}\omega_i)$ is skew-symmetric. Without loss of generality, the control torque $\mathbf{u}$ generated by momentum wheels ($\dot{\gamma} = 0$) can be defined as $\mathbf{u}_i = -\dot{\mathbf{h}}_i$. Then, the $\mathbf{S}(\mathbf{J}_{\mathbf{s/c},i}\omega_i)$ in (7) is replaced by $\mathbf{S}(\mathbf{J}_{\mathbf{s/c},i}\omega_i + \mathbf{h}_i)$ in order to account for the gyro stiffening effect of the wheels.

In the subsequent sections, the rotational dynamics formulation in (5) is used to develop a nonlinear synchronization tracking control law for multiple formation flying spacecraft.

C. Relative Translational Dynamics

If we assume that the influence of the attitude dynamics on the translational dynamics is weak and ignored, the translational dynamics, modeled as double integrators,[7] can be easily augmented with the attitude dynamics in (5). Alternatively, similar to Ref. 13, 33, the coupled translational and rotational motions of formation spacecraft can be written in the Lagrangian form in (2). Then, the proposed decentralized tracking control can be effectively applied without loss of generality. For arbitrary translational dynamics, synchronization corresponds to $\mathbf{x}_1 = \mathbf{x}_2 = \cdots = \mathbf{x}_p$ where $\mathbf{x}_i$, $1 \leq i \leq p$ connotes a vector of biased variables constructed from the position vector $\mathbf{r}_i$ such that $\mathbf{r}_i(t) = \mathbf{x}_i(t) + \mathbf{b}_i(t)$ and the separation vector $\mathbf{b}_i(t)$ is independent of the dynamics.[4] Conceptually, such a method follows that each position vector $\mathbf{x}_i$ can be defined from virtually shifted origins. In this paper, the goal is to take a different approach in which the phase differences of the position variables can synchronize on a spiral or circular trajectory.

In pursuit of this goal, this section presents relative translational dynamics applicable to formation flight on a circular or spiral configuration in low earth orbit (LEO) such that the formation translational control is based on the relative dynamics with respect to the desired formation center of mass (c.m.). For deriving a relative position control law, it is more advantageous to work in the non-inertial orbital coordinates F^{RO} as illustrated in Fig. 1. The orbital frame F^{RO} is defined in such a way that its origin is attached to the center of mass of the formation with its y-axis aligned with the position vector $\mathbf{R}_0$ representing the position of the formation center of mass in the Earth Centered Inertial (ECI) frame. The z-axis points towards the orbital plane normal and the x-axis completes the right hand system (see Fig. 1).

Although this derivation can also be done in an orbital frame attached to the *leader* satellite, the leader satellite will be maneuvering in general so its orbital velocity would not be a constant. Therefore, it is more

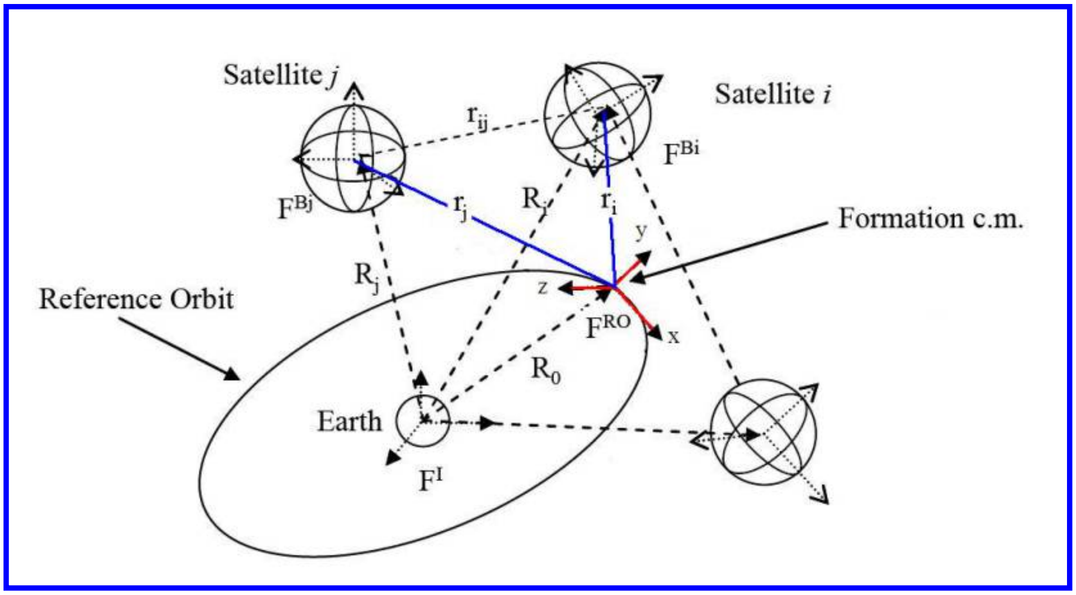

Figure 1. Geometry of different reference frames

accurate to use an orbital reference frame attached to the center of mass of the formation as opposed to the leader satellite.

For simplicity, we will assume a circular reference orbit for the formation center of mass for which the angular velocity of the reference orbit is simply:

$$\omega_0 = \sqrt{\frac{\mu_e}{R_0^3}} \tag{9}$$

where μ_e is the gravitational constant of Earth ($398,600.4418 \times 10^9$ $\mathrm{m}^3/\mathrm{s}^2$) and R_0 is the radius of the formation's center of mass orbit.

Even though we consider the J2 effects as a source of disturbance for simulation studies in this paper, we ignore the J2 terms for the control law development. Then, the relative dynamics of i-th satellite with respect to satellite-k in the orbital frame F^{RO} can be written as[3]

$$\begin{aligned} \ddot{x}_i - 2\omega_0\dot{y}_i - {\omega_0}^2 x_i + \frac{\mu_e x_i}{R_i^3} &= \frac{F_x + F_{xd}}{m} \\ \ddot{y}_i + 2\omega_0\dot{x}_i - {\omega_0}^2 y_i + \frac{\mu_e(R_0 + y_i)}{R_i^3} - \frac{\mu_e}{R_0^2} &= \frac{F_y + F_{yd}}{m} \\ \ddot{z}_i + \frac{\mu_e z_i}{R_i^3} &= \frac{F_z + F_{zd}}{m} \end{aligned} \tag{10}$$

where F_x, F_y, and F_z denote the control forces while F_{xd}, F_{yd}, and F_{zd} represent the external disturbance forces, all expressed in the orbital frame F^{RO}. In addition, the distance between the Earth center and the i-th satellite is defined as

$$R_i = \sqrt{x_i^2 + (y_i + R_0)^2 + z_i^2} \tag{11}$$

If R_i is sufficiently close to R_0, (10) reduces to Clohessy-Wiltshire equations (also called Hill's equation).

Ignoring the disturbances, (10) can be written in a Lagrangian form with a constant mass matrix, similar to (2)

$$\mathbf{M}\ddot{\mathbf{r}}_i + \mathbf{C}\dot{\mathbf{r}}_i + \mathbf{D}(\mathbf{r}_i)\mathbf{r}_i + \mathbf{g}(\mathbf{r}_i) = \mathbf{F}_i \tag{12}$$

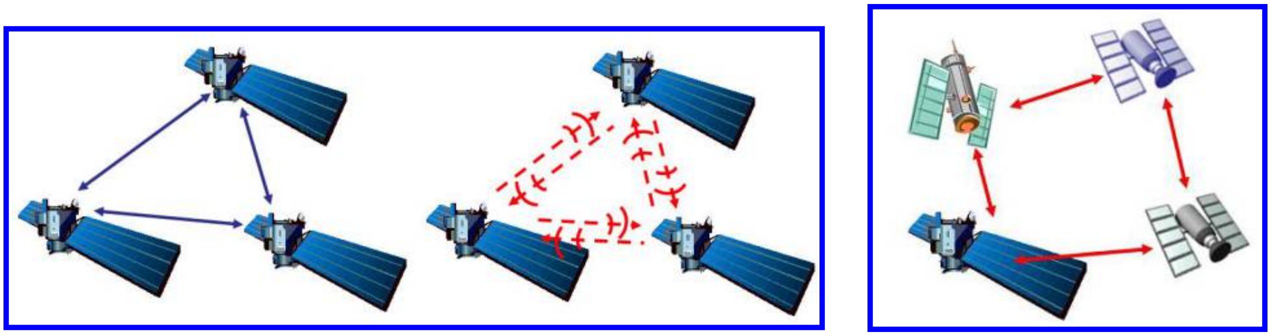

(a) network of identical spacecraft via communication coupling (left) or relative sensing (right)

(b) non-identical spacecraft

Figure 2. Multi-agent networks of identical or nonidentical spacecraft using local couplings. They are on balanced bi-directional graphs, but a more complex geometry or leader-follower network can also be constructed by concurrent synchronization.[17] Also, without loss of generality, the bi-directional couplings can be extended to uni-directional couplings.[17]

where

$$\mathbf{M}=\begin{bmatrix} m & 0 & 0\\ 0 & m & 0\\ 0 & 0 & m\end{bmatrix},\quad \mathbf{r}_i=\begin{pmatrix} x_i\\ y_i\\ z_i\end{pmatrix},\quad \mathbf{C}=\begin{bmatrix} 0 & -2m\omega_0 & 0\\ 2m\omega_0 & 0 & 0\\ 0 & 0 & 0\end{bmatrix},\quad \mathbf{F}_i=\begin{pmatrix} F_x\\ F_y\\ F_z\end{pmatrix}$$
$$\mathbf{D}(\mathbf{r}_i)=\begin{bmatrix} -m\omega_0^2+m\frac{\mu_e}{R_i^3} & 0 & 0\\ 0 & -m\omega_0^2+m\frac{\mu_e}{R_i^3} & 0\\ 0 & 0 & \frac{\mu_e}{R_i^3}\end{bmatrix},\qquad \mathbf{g}(\mathbf{r}_i)=\begin{pmatrix} 0\\ m\left(\frac{\mu_e R_0}{R_i^3}-\frac{\mu_e}{R_0^2}\right)\\ 0\end{pmatrix} \tag{13}$$

We make two important remarks regarding (12). First, as opposed to the attitude dynamics of spacecraft in the preceding section, $\mathbf{M}$ and $\mathbf{C}$ are constant, which simplifies the stability proofs. Nonetheless, $\dot{\mathbf{M}}-2\mathbf{C}$ is skew-symmetric, which unifies our control law design for both attitude and translational dynamics. Note that the $\mathbf{C}$ matrix in (12) is not obtained from (3). Second, for practical applications, the difference between R_i and R_0 is reasonably small, resulting in $\mathbf{D}(\mathbf{r}_i)=\mathbf{D}=\mathrm{diag}(0,0,\omega_0^2)$. This will further simplify the proposed control law in Sec. IV.

III. Decentralized Nonlinear Control for Attitude Synchronization

We consider the attitude synchronization of multiple spacecraft following a common time-varying trajectory in this section.

A. Attitude Synchronization of Spacecraft

The following decentralized tracking control law with two-way-ring symmetry is proposed for the i-th spacecraft in the network comprised of p spacecraft (see Figure 2(a)):

$$\tau_i=\mathbf{M}_i(\mathbf{q}_i)\ddot{\mathbf{q}}_{r,i}+\mathbf{C}_i(\mathbf{q}_i,\dot{\mathbf{q}}_i)\dot{\mathbf{q}}_{r,i}+\mathbf{g}_i(\mathbf{q}_i)-\mathbf{K}_1\mathbf{s}_i+\mathbf{K}_2\mathbf{s}_{i-1}+\mathbf{K}_2\mathbf{s}_{i+1} \tag{14}$$

where a positive-definite matrix $\mathbf{K}_1\in\mathbb{R}^{n\times n}$ is a feedback gain for the i-th satellite, and another positive-definite matrix $\mathbf{K}_2\in\mathbb{R}^{n\times n}$ is a coupling gain with the adjacent members ($i-1$ and $i+1$). For two-spacecraft networks, the last coupling term with the $i+1$-th member in (14) is not used. It should be emphasized that the assumption of the bi-directional coupling in (14) can be relaxed without loss of generality to account for a regular digraph.[17] Also, $\dot{\mathbf{q}}_{r,i}$ and $\mathbf{s}_i$ are defined such that

$$\dot{\mathbf{q}}_{r,i}=\dot{\mathbf{q}}_d(t)+\mathbf{\Lambda}(\mathbf{q}_d(t)-\mathbf{q}_i),\quad \mathbf{s}_i=\dot{\mathbf{q}}_i-\dot{\mathbf{q}}_{r,i}=\dot{\mathbf{q}}_i-\dot{\mathbf{q}}_d(t)+\mathbf{\Lambda}(\mathbf{q}_i-\mathbf{q}_d(t)) \tag{15}$$

where $\mathbf{\Lambda}$ is a positive diagonal matrix. The time-varying desired trajectory $\mathbf{q}_d(t)$ can be the formation flying guidance command or the trajectory of a leader spacecraft.

If we assume that a relative attitude metrology system, similar to Ref. 35, is available in addition to each spacecraft's own attitude measurement with respect to the inertial frame, the relative attitude errors (e.g., $\mathbf{q}_{i+1}-\mathbf{q}_i$) can be computed. In turn, nonlinear observers can estimate the velocity errors (e.g., $\dot{\mathbf{q}}_{i+1}-\dot{\mathbf{q}}_i$), we can rewrite (14) as

$$\begin{aligned}\tau_i =&\mathbf{M}_i(\mathbf{q}_i)\ddot{\mathbf{q}}_{r,i}+\mathbf{C}_i(\mathbf{q}_i,\dot{\mathbf{q}}_i)\dot{\mathbf{q}}_{r,i}+\mathbf{g}_i(\mathbf{q}_i)-(\mathbf{K}_1-2\mathbf{K}_2)\mathbf{s}_i\\ &+\mathbf{K}_2\left[(\dot{\mathbf{q}}_{i-1}-\dot{\mathbf{q}}_i)+\mathbf{\Lambda}(\mathbf{q}_{i-1}-\mathbf{q}_i)\right]+\mathbf{K}_2\left[(\dot{\mathbf{q}}_{i+1}-\dot{\mathbf{q}}_i)+\mathbf{\Lambda}(\mathbf{q}_{i+1}-\mathbf{q}_i)\right]\end{aligned} \tag{16}$$

This can be straightforwardly applied to the translational dynamics with relative distance measurements,[36] as shall be seen in Section IV. This implies that such a relative sensing system can eliminate the need for exchanging the state information of each spacecraft; no inter-satellite communication would be required. In essence, we can implement the proposed decentralized control law by either the communication links or the relative metrology system, as illustrated in Fig. 2.

It should be noted again that one of the main contributions of this paper lies with the use of a new differential stability framework, yielding the exact proof of nonlinear stability under a variety of conditions, while many others can still come up with nonlinear control laws similar to (14), without a rigorous stability proof. Note that the above control law requires only the coupling feedback of the most adjacent spacecraft ($i-1$ and $i+1$) for exponential convergence (see Figure 2). Consequently, the last (p-th) satellite is connected with the first satellite to form a ring network as suggested in Ref. 23. In order to construct a more complex geometry rather than a ring network, concurrent synchronization[32] can be used, as expanded upon in Ref. 4, 17.

Without loss of generality, we can extend the proposed control law to adaptive control[18]

$$\begin{aligned}\tau_i &= \mathbf{Y}_i\hat{\mathbf{a}}_i-\mathbf{K}_1\mathbf{s}_i+\mathbf{K}_2\mathbf{s}_{i-1}+\mathbf{K}_2\mathbf{s}_{i+1}\\ &=\hat{\mathbf{M}}_i\ddot{\mathbf{q}}_{r,i}+\hat{\mathbf{C}}_i\dot{\mathbf{q}}_{r,i}+\hat{\mathbf{g}}_i(\mathbf{q}_i)-\mathbf{K}_1\mathbf{s}_i+\mathbf{K}_2\mathbf{s}_{i-1}+\mathbf{K}_2\mathbf{s}_{i+1}\end{aligned} \tag{17}$$

The parameter estimate $\hat{\mathbf{a}}_i$ for the i-th member is updated by the correlation integral:

$$\dot{\hat{\mathbf{a}}}_i = -\mathbf{\Gamma}\mathbf{Y}_i^T\mathbf{s}_i \tag{18}$$

where $\mathbf{\Gamma}$ is a symmetric positive definite matrix. The stability proof of the adaptive control law, presented in Refs. 4, 17, does not alter the main proofs in this paper except that the convergence result reduces to asymptotic in stead of exponential. Hence, we will only focus on the general control law in (2) for the sake of simplicity.

The closed-loop dynamics for the whole formation, by using (2) and (14), can be written as

$$[\mathbf{M}]\dot{\mathbf{x}}+[\mathbf{C}]\mathbf{x}+[\mathbf{L}^p_{\mathbf{K}_1,-\mathbf{K}_2}]\mathbf{x}=\mathbf{0} \tag{19}$$

where

$$[\mathbf{M}]=\begin{bmatrix}\mathbf{M}_1(\mathbf{q}_1) & \cdots & \mathbf{0}\\ \vdots & \ddots & \vdots\\ \mathbf{0} & \cdots & \mathbf{M}_p(\mathbf{q}_p)\end{bmatrix},\quad [\mathbf{C}]=\begin{bmatrix}\mathbf{C}_1(\mathbf{q}_1,\dot{\mathbf{q}}_1) & \cdots & \mathbf{0}\\ \vdots & \ddots & \vdots\\ \mathbf{0} & \cdots & \mathbf{C}_p(\mathbf{q}_p,\dot{\mathbf{q}}_p)\end{bmatrix},\quad \mathbf{x}=\begin{pmatrix}\mathbf{s}_1\\ \vdots\\ \mathbf{s}_p\end{pmatrix} \tag{20}$$

Also, the $pn\times pn$ block matrix $[\mathbf{L}^p_{\mathbf{K}_1,-\mathbf{K}_2}]$ has $\mathbf{K}_1$ as its diagonal matrix elements, neighbored by $-\mathbf{K}_2$. In other words, from the definition of the controller in (14), $[\mathbf{L}^p_{\mathbf{K}_1,-\mathbf{K}_2}]$ has only three nonzero matrix elements in each row (i.e., $\mathbf{K}_1,\mathbf{K}_2,\mathbf{K}_2$).

The network graphs illustrated in Figure 2 are *balanced* due to bi-directional coupling.[9] However, it should be noted that the matrix $[\mathbf{L}^p_{\mathbf{K}_1,-\mathbf{K}_2}]$ is different from the standard weighted Laplacian found in Ref. 9. By definition, every row sum of the Laplacian matrix is zero. Hence, the Laplacian matrix always has a zero eigenvalue corresponding to a right eigenvector, $\mathbf{1}=(1,1,\cdots,1)^T$.[9] In contrast, a strictly positive definite $[\mathbf{L}^p_{\mathbf{K}_1,-\mathbf{K}_2}]$ is required for exponential convergence for the proposed control law in this paper.

We present the main theorems of the paper. First, the following condition should be true for exponential convergence to a common desired trajectory $\mathbf{q}_d(t)$.

Theorem III.1 ***Global Exponential Convergence to the Desired Trajectory***
If $[\mathbf{L}^p_{\mathbf{K}_1,-\mathbf{K}_2}]$ is uniformly positive definite, then every member of the network follows the desired trajectory $\mathbf{q}_d$ exponentially fast regardless of initial conditions. In other words, if $\mathbf{K}_1 - 2\mathbf{K}_2 > 0$, then $\mathbf{q}_i$, ($i = 1, 2, \cdots, p$, $p \geq 3$) converges to $\mathbf{q}_d$ exponentially fast from any initial conditions. For two-spacecraft systems ($p = 2$), $\mathbf{K}_1 - \mathbf{K}_2 > 0$ needs to be true instead.

Proof We present a new proof that emphasizes the hierarchical combination structure of the proposed control law. The equation (19) of the closed-loop dynamics corresponds to a conventional tracking problem.

Recalling Theorem VI.2, we construct the following hierarchical virtual system of $\mathbf{y}_1$ and $\mathbf{y}_2$:

$$\begin{bmatrix} [\mathbf{M}] & \mathbf{0} \\ \mathbf{0} & \mathbf{I} \end{bmatrix} \begin{pmatrix} \dot{\mathbf{y}}_1 \\ \dot{\mathbf{y}}_2 \end{pmatrix} + \begin{bmatrix} [\mathbf{C}] + [\mathbf{L}^p_{\mathbf{K}_1,-\mathbf{K}_2}] & \mathbf{0} \\ -\mathbf{I} & [\mathbf{\Lambda}] \end{bmatrix} \begin{pmatrix} \mathbf{y}_1 \\ \mathbf{y}_2 \end{pmatrix} = \begin{pmatrix} \mathbf{0} \\ \mathbf{0} \end{pmatrix} \tag{21}$$

where the virtual system of $\mathbf{y}_1$ is obtained by replacing $\mathbf{x}$ with $\mathbf{y}_1$ in (19), and the system of $\mathbf{y}_2$ is from the definition of the composite variable in (15). Also, $[\mathbf{\Lambda}] = \mathrm{diag}(\mathbf{\Lambda}, \cdots, \mathbf{\Lambda})$.

It is straightforward to verify that (21) has two particular solutions:

$$\begin{pmatrix} \mathbf{y}_1 = \mathbf{x} \\ \mathbf{y}_2 = \{\tilde{\mathbf{q}}\} \end{pmatrix} \quad \text{and} \quad \begin{pmatrix} \mathbf{y}_1 = \mathbf{0} \\ \mathbf{y}_2 = \mathbf{0} \end{pmatrix}, \text{ where } \{\tilde{\mathbf{q}}\} = \begin{pmatrix} \mathbf{q}_1 - \mathbf{q}_d \\ \vdots \\ \mathbf{q}_p - \mathbf{q}_d \end{pmatrix} \tag{22}$$

The differential virtual length analysis with respect to the uniformly positive definite metric,

$$\begin{bmatrix} [\mathbf{M}] & \mathbf{0} \\ \mathbf{0} & \alpha\mathbf{I} \end{bmatrix}, \quad \exists \alpha > 0 \tag{23}$$

yields

$$\begin{aligned} \frac{d}{dt} \begin{pmatrix} \delta\mathbf{y}_1 \\ \delta\mathbf{y}_2 \end{pmatrix}^T \begin{bmatrix} [\mathbf{M}] & \mathbf{0} \\ \mathbf{0} & \alpha\mathbf{I} \end{bmatrix} \begin{pmatrix} \delta\mathbf{y}_1 \\ \delta\mathbf{y}_2 \end{pmatrix} &= \begin{pmatrix} \delta\mathbf{y}_1 \\ \delta\mathbf{y}_2 \end{pmatrix}^T \begin{bmatrix} [\dot{\mathbf{M}}] & \mathbf{0} \\ \mathbf{0} & \mathbf{0} \end{bmatrix} \begin{pmatrix} \delta\mathbf{y}_1 \\ \delta\mathbf{y}_2 \end{pmatrix} + 2 \begin{pmatrix} \delta\mathbf{y}_1 \\ \delta\mathbf{y}_2 \end{pmatrix}^T \begin{bmatrix} [\mathbf{M}] & \mathbf{0} \\ \mathbf{0} & \alpha\mathbf{I} \end{bmatrix} \begin{pmatrix} \delta\dot{\mathbf{y}}_1 \\ \delta\dot{\mathbf{y}}_2 \end{pmatrix} \\ &= \begin{pmatrix} \delta\mathbf{y}_1 \\ \delta\mathbf{y}_2 \end{pmatrix}^T \begin{bmatrix} [\dot{\mathbf{M}}] & \mathbf{0} \\ \mathbf{0} & \mathbf{0} \end{bmatrix} \begin{pmatrix} \delta\mathbf{y}_1 \\ \delta\mathbf{y}_2 \end{pmatrix} + 2 \begin{pmatrix} \delta\mathbf{y}_1 \\ \delta\mathbf{y}_2 \end{pmatrix}^T \begin{bmatrix} -[\mathbf{C}] - [\mathbf{L}^p_{\mathbf{K}_1,-\mathbf{K}_2}] & \mathbf{0} \\ \alpha\mathbf{I} & -\alpha[\mathbf{\Lambda}] \end{bmatrix} \begin{pmatrix} \delta\mathbf{y}_1 \\ \delta\mathbf{y}_2 \end{pmatrix} \\ &= \begin{pmatrix} \delta\mathbf{y}_1 \\ \delta\mathbf{y}_2 \end{pmatrix}^T \begin{bmatrix} -2[\mathbf{L}^p_{\mathbf{K}_1,-\mathbf{K}_2}] & \mathbf{0} \\ 2\alpha\mathbf{I} & -2\alpha[\mathbf{\Lambda}] \end{bmatrix} \begin{pmatrix} \delta\mathbf{y}_1 \\ \delta\mathbf{y}_2 \end{pmatrix} = \begin{pmatrix} \delta\mathbf{y}_1 \\ \delta\mathbf{y}_2 \end{pmatrix}^T \mathbf{B} \begin{pmatrix} \delta\mathbf{y}_1 \\ \delta\mathbf{y}_2 \end{pmatrix} \end{aligned} \tag{24}$$

where we used the skew-symmetric property of $[\dot{\mathbf{M}}] - 2[\mathbf{C}]$.

The symmetric part of the matrix $\mathbf{B}$ is

$$\mathbf{B}_s = \frac{1}{2}(\mathbf{B} + \mathbf{B}^T) = \begin{bmatrix} -2[\mathbf{L}^p_{\mathbf{K}_1,-\mathbf{K}_2}] & \alpha\mathbf{I} \\ \alpha\mathbf{I} & -2\alpha[\mathbf{\Lambda}] \end{bmatrix} \tag{25}$$

According to Theorem VI.1, (21) is contracting if the symmetric matrix $\mathbf{B}_s$ is uniformly negative definite. We can always find $\alpha > 0$ such that $\mathbf{B}_s$ is uniformly negative definite:

$$\alpha\mathbf{I} < 4[\mathbf{L}^p_{\mathbf{K}_1,-\mathbf{K}_2}][\mathbf{\Lambda}], \quad [\mathbf{L}^p_{\mathbf{K}_1,-\mathbf{K}_2}] > 0, \quad \text{and} \quad \mathbf{\Lambda} > 0 \tag{26}$$

Accordingly, all solutions of (21) converge to each exponentially fast, resulting in synchronization of $\mathbf{q}$ with $\mathbf{q}_d(t)$. The positive-definiteness of $[\mathbf{L}^p_{\mathbf{K}_1,-\mathbf{K}_2}]$ corresponds to $\mathbf{K}_1 - \mathbf{K}_2 > 0$ for two-spacecraft systems ($p = 2$). For a network consisting of more than two spacecraft ($p \geq 3$), it can be shown that $\mathbf{K}_1 - 2\mathbf{K}_2$ is a sufficient condition of the positive-definiteness of $[\mathbf{L}^p_{\mathbf{K}_1,-\mathbf{K}_2}]$ given $\mathbf{K}_1 > 0, \mathbf{K}_2 > 0$.

We now focus on the synchronization of multiple spacecraft dynamics. First, we introduce an orthogonal matrix, whose column vectors constitute a superset of the flow-invariant subspace of synchronization[17,32] such that $\mathbf{V}^T_{sync}\mathbf{x} = 0$.

Since $[\mathbf{L}^p_{\mathbf{K}_1,-\mathbf{K}_2}]$ is a constant real symmetric matrix, we can perform the spectral decomposition

$$[\mathbf{L}^p_{\mathbf{K}_1,-\mathbf{K}_2}] = \mathbf{V}[\mathbf{D}]\mathbf{V}^T, \quad [\mathbf{D}] = \mathbf{V}^T[\mathbf{L}^p_{\mathbf{K}_1,-\mathbf{K}_2}]\mathbf{V} \tag{27}$$

where $[\mathbf{D}]$ is a block diagonal matrix, and the square matrix $\mathbf{V}$ is composed of the orthonormal eigenvectors. Since the symmetry of $[\mathbf{L}^p_{\mathbf{K}_1,-\mathbf{K}_2}]$ gives rise to real eigenvalues and orthonormal eigenvectors,[34] we can verify that $\mathbf{V}^T\mathbf{V} = \mathbf{V}\mathbf{V}^T = \mathbf{I}_{pn}$,

The modified Laplacian $[\mathbf{L}^p_{\mathbf{K}_1,-\mathbf{K}_2}]$ defines a *regular* graph, where each member has the same number of neighbors ($= 2$ for $p \geq 3$). A regular graph has the block column identify matrix $[\mathbf{1}] = [\mathbf{I}_n, \mathbf{I}_n, \cdots, \mathbf{I}_n]^T/\sqrt{p}$ as its eigenvectors associated with the tracking convergence rate $\lambda(\mathbf{K}_1 - 2\mathbf{K}_2)$ for $p \geq 3$. Hence, we can define a $pn \times (p-1)n$ matrix $\mathbf{V}_{sync}$ constructed from the orthonormal eigenvectors other than $[\mathbf{1}]$ such that

$$\mathbf{V}^T\mathbf{V} = \begin{pmatrix} [\mathbf{1}]^T \\ \mathbf{V}^T_{sync} \end{pmatrix} \begin{pmatrix} [\mathbf{1}] & \mathbf{V}_{sync} \end{pmatrix} = \begin{bmatrix} [\mathbf{1}]^T[\mathbf{1}] & [\mathbf{1}]^T\mathbf{V}_{sync} \\ \mathbf{V}^T_{sync}[\mathbf{1}] & \mathbf{V}^T_{sync}\mathbf{V}_{sync} \end{bmatrix} = \begin{bmatrix} \mathbf{I}_n & \mathbf{0}_{n\times(p-1)n} \\ \mathbf{0}_{(p-1)n\times n} & \mathbf{I}_{(p-1)n} \end{bmatrix} \tag{28}$$

where we used the orthogonality between $[\mathbf{1}]$ and $\mathbf{V}_{sync}$.

The synchronization of multiple spacecraft $\mathbf{q}_1 = \mathbf{q}_2 = \cdots = \mathbf{q}_p$ corresponds to

$$V^T_{sync} \begin{pmatrix} \mathbf{q}_1 \\ \vdots \\ \mathbf{q}_p \end{pmatrix} = \mathbf{0} \tag{29}$$

.

Theorem III.2 ***Synchronization of Multiple Identical or Heterogeneous Spacecraft***
A network of p spacecraft synchronize exponentially from any initial conditions if $\exists$ diagonal matrices $\mathbf{K}_1 > 0$, $\mathbf{K}_2 > 0$ such that

$$\mathbf{V}^T_{sync}[\mathbf{L}^p_{\mathbf{K}_1,-\mathbf{K}_2}]\mathbf{V}_{sync} > 0$$

In addition, $\mathbf{\Lambda}$ is a positive diagonal matrix defining a stable composite variable $\mathbf{s}_i = \dot{\widetilde{\mathbf{q}}}_i + \mathbf{\Lambda}\widetilde{\mathbf{q}}_i$ with $\widetilde{\mathbf{q}}_i = \mathbf{q}_i - \mathbf{q}_d(t)$.

If we have uni-directional couplings on a regular graph, the preceding conditions is replaced by

$$\mathbf{V}^T_{sync}\left([\mathbf{L}^p_{\mathbf{K}_1,-\mathbf{K}_2}] + [\mathbf{L}^p_{\mathbf{K}_1,-\mathbf{K}_2}]^T\right)\mathbf{V}_{sync} > 0 \tag{30}$$

(see Ref. 17 for details). This theorem corresponds to synchronization with stable tracking. Multiple dynamics need not be identical to achieve stable synchronization. It should be noted that Theorem III.2 can hold, regardless of Theorem III.1. For example, $[\mathbf{L}^p_{\mathbf{K}_1,-\mathbf{K}_2}]$ might be semi-positive definite, thus yielding indifferent tracking dynamics. In this case, we do not need a common reference trajectory for the synchronization of multiple spacecraft, and the spacecraft synchronize to the average of the initial conditions (see Ref. 17 for details). It is useful to note that the above condition corresponds to $\mathbf{K}_1 + \mathbf{K}_2 > 0$ for two-spacecraft and three-spacecraft networks ($p = 2, 3$).

Note that we can render the system synchronized first, then follow the common trajectory by tuning the gains properly. This indicates that there exist two different time-scales in the closed-loop systems constructed with the proposed controllers. For two-spacecraft systems, the convergence of exponential tracking is proportional to $\mathbf{K}_1 - \mathbf{K}_2$ whereas the synchronization has a convergence rate of $\mathbf{K}_1 + \mathbf{K}_2$. This multi-time-scale behavior will be exploited in the subsequent sections.

B. Proof of Exponential Synchronization

We summarize the proof of Theorem III.2 for the exponential synchronization of multiple nonlinear dynamics, first reported in Ref. 17. The key result can be generalized for an arbitrary number of spacecraft, even to more complex structures beyond a standard ring geometry.[17]

Suppose that $\mathbf{M}(\mathbf{q})$ is a constant inertia matrix $\mathbf{M}$, thereby resulting in $\mathbf{C}(\mathbf{q}, \dot{\mathbf{q}}) = 0$. Then, we can easily prove $\mathbf{s}_1$ and $\mathbf{s}_2$ tend to each other using Theorem VI.4. On the other hand, the difficulties associated with nonlinear time-varying inertia matrices can be easily demonstrated (see Ref. 17). In essence, $\mathbf{M}(\mathbf{q}_1) \neq \mathbf{M}(\mathbf{q}_2)$ makes this problem intractable in general. We now present a solution to this open problem, focused on the synchronization of multiple spacecraft with non-constant nonlinear metrics.

Recall the closed-loop dynamics given in (19). Pre-multiplying (19) by $\mathbf{V}^T$ and setting $\mathbf{x} = \mathbf{V}\mathbf{V}^T\mathbf{x}$ result in

$$\left(\mathbf{V}^T[\mathbf{M}]\mathbf{V}\right)\dot{\mathbf{z}} + \left(\mathbf{V}^T[\mathbf{C}]\mathbf{V}\right)\mathbf{z} + [\mathbf{D}]\mathbf{z} = \mathbf{0} \tag{31}$$

where $\mathbf{z} = \mathbf{V}^T\mathbf{x}$.

Then, we can develop the squared-length analysis similar to (24). Notice that $\left(\mathbf{V}^T[\mathbf{M}]\mathbf{V}\right)$ is always symmetric positive definite since $[\mathbf{M}]$ is symmetric positive definite.

Using (28), the block diagonal matrix $[\mathbf{D}]$, which represents the eigenvalues of $[\mathbf{L}^p_{\mathbf{K}_1,-\mathbf{K}_2}]$, can be partitioned from (27)

$$\mathbf{V}^T[\mathbf{L}^p_{\mathbf{K}_1,-\mathbf{K}_2}]\mathbf{V} = \begin{bmatrix} [\mathbf{1}]^T[\mathbf{L}^p_{\mathbf{K}_1,-\mathbf{K}_2}][\mathbf{1}] & [\mathbf{1}]^T[\mathbf{L}^p_{\mathbf{K}_1,-\mathbf{K}_2}]\mathbf{V}_{sync} \\ \mathbf{V}^T_{sync}[\mathbf{L}^p_{\mathbf{K}_1,-\mathbf{K}_2}][\mathbf{1}] & \mathbf{V}^T_{sync}[\mathbf{L}^p_{\mathbf{K}_1,-\mathbf{K}_2}]\mathbf{V}_{sync} \end{bmatrix} = \begin{bmatrix} \mathbf{D}_1 & \mathbf{0}_{n\times(p-1)n} \\ \mathbf{0}_{(p-1)n\times n} & \mathbf{D}_2 \end{bmatrix} \tag{32}$$

It should be noted that $\mathbf{D}_1 = \mathbf{K}_1 - 2\mathbf{K}_2$ for $p \geq 3$ (or $\mathbf{D}_1 = \mathbf{K}_1 - \mathbf{K}_2$ for $p = 2$) represents the tracking gain while $\mathbf{D}_2$ corresponds to the synchronization gain. We can choose the control gain matrices $\mathbf{K}_1$ and $\mathbf{K}_2$ such that

$$\mathbf{D}_2 = \mathbf{V}^T_{sync}[\mathbf{L}^p_{\mathbf{K}_1,-\mathbf{K}_2}]\mathbf{V}_{sync} > \mathbf{D}_1 = [\mathbf{1}]^T[\mathbf{L}^p_{\mathbf{K}_1,-\mathbf{K}_2}][\mathbf{1}] \tag{33}$$

This will ensure that multiple spacecraft synchronize faster than they follow the common desired trajectory. In other words, multiple spacecraft synchronize first, then they converge to the desired trajectory while staying together.

Now let us write the virtual system of $\mathbf{y}$ by replacing $\mathbf{z}$ in (31) with $\mathbf{y}$.

$$\left(\mathbf{V}^T[\mathbf{M}]\mathbf{V}\right)\dot{\mathbf{y}} + \left(\mathbf{V}^T[\mathbf{C}]\mathbf{V}\right)\mathbf{y} + [\mathbf{D}]\mathbf{y} = \mathbf{0} \tag{34}$$

The above system has the following particular solutions:

$$\mathbf{y} = \begin{pmatrix} \mathbf{y}_t \\ \mathbf{y}_s \end{pmatrix} = \begin{pmatrix} [\mathbf{1}]^T\mathbf{x} \\ \mathbf{V}^T_{sync}\mathbf{x} \end{pmatrix} \quad \text{and} \quad \mathbf{y} = \begin{pmatrix} \mathbf{y}_t \\ \mathbf{y}_s \end{pmatrix} = \begin{pmatrix} \mathbf{0} \\ \mathbf{0} \end{pmatrix} \tag{35}$$

Now we need to prove that the system in (34) is contracting (i.e., $\delta\mathbf{y} \rightarrow \mathbf{0}$ globally and exponentially) in order to show that those two solutions tend exponentially to each other. Performing the squared-length analysis with respect to the symmetric positive definite block matrix $\mathbf{V}^T[\mathbf{M}]\mathbf{V}$ as the contraction metric yields

$$\frac{d}{dt}\begin{pmatrix} \delta\mathbf{y}_t \\ \delta\mathbf{y}_s \end{pmatrix}^T \begin{bmatrix} [\mathbf{1}]^T[\mathbf{M}][\mathbf{1}] & [\mathbf{1}]^T[\mathbf{M}]\mathbf{V}_{sync} \\ \mathbf{V}^T_{sync}[\mathbf{M}][\mathbf{1}] & \mathbf{V}^T_{sync}[\mathbf{M}]\mathbf{V}_{sync} \end{bmatrix} \begin{pmatrix} \delta\mathbf{y}_t \\ \delta\mathbf{y}_s \end{pmatrix} = -2\begin{pmatrix} \delta\mathbf{y}_t \\ \delta\mathbf{y}_s \end{pmatrix}^T \begin{bmatrix} \mathbf{D}_1 & \mathbf{0} \\ \mathbf{0} & \mathbf{D}_2 \end{bmatrix} \begin{pmatrix} \delta\mathbf{y}_t \\ \delta\mathbf{y}_s \end{pmatrix} \tag{36}$$

where we used the skew-symmetric property of $\left(\mathbf{V}^T[\dot{\mathbf{M}}]\mathbf{V}\right) - 2\left(\mathbf{V}^T[\mathbf{C}]\mathbf{V}\right)$.

If $[\mathbf{D}] > 0$, or equivalently $[\mathbf{L}^p_{\mathbf{K}_1,-\mathbf{K}_2}] > 0$, the combined virtual system in (34) is contracting. This in turn implies that all solutions of $\mathbf{y}$ tend to a single trajectory. As a result, $[\mathbf{1}]^T\mathbf{x} = (\mathbf{s}_1 + \cdots + \mathbf{s}_p)/\sqrt{p}$ and $\mathbf{V}^T_{sync}\mathbf{x}$ tend exponentially to zero. Note that $\mathbf{s}_1, \cdots, \mathbf{s}_p \rightarrow \mathbf{0}$ has already been proven for Theorem III.1. What is new here is the proof of synchronization $\mathbf{V}^T_{sync}\mathbf{x} \rightarrow \mathbf{0}$.

By exploiting the hierarchical structure (Theorem VI.2) of the composite variable defined in (15), we can show that $\mathbf{V}^T_{sync}\mathbf{x} \rightarrow \mathbf{0}$ and $\mathbf{\Lambda} > 0$ also make $\mathbf{q}_1, \cdots, \mathbf{q}_p$ synchronize exponentially (i.e., $\mathbf{V}^T_{sync}\left(\mathbf{q}_1^T, \cdots, \mathbf{q}_p^T\right)^T \rightarrow \mathbf{0}$). This straightforwardly follows the proof of Theorem III.1.

In the case of identical spacecraft, this synchronization result also implies that the diagonal terms of the metric, $\mathbf{V}^T_{sync}[\mathbf{M}][\mathbf{1}]$ tend to zero exponentially, thereby eliminating the coupling of the inertia term $\mathbf{V}^T[\mathbf{M}]\mathbf{V}$ in (36). So far, we have assumed that $\mathbf{q}_d(t)$ is identical for each spacecraft. If $\mathbf{q}_d(t)$ were different for each dynamics, $\mathbf{s}_i \rightarrow \mathbf{s}_j$ would imply the synchronization of $\mathbf{q}_i - \mathbf{q}_j$ to the difference of the desired trajectories, which would be useful to construct phase synchronization of spacecraft positions. Such phase synchronization is discussed in the subsequent section. It should be mentioned that global asymptotic convergence of a linear coupling control law for the nonlinear attitude dynamics is proven in Ref. 17, and compared with the proposed nonlinear control law in Sec. V.

IV. Decentralized Nonlinear Control for Relative Translational Dynamics

We introduce a new method for the phase synchronization of multiple spacecraft positions that follow a time-varying circular or spiral trajectory with equal spacing between spacecraft, as shown in Figure 3. We also illustrate that the rotational and translational dynamics can be combined to enable coupled rotational maneuvers, which can realize a spiral trajectory. The UV coverage of an interferometer defines the size and density of spatial points on the two-dimensional Modulation Transfer Function (MTF) of an image.[4,5] By spiraling out, a stellar interferometer can construct a virtually large telescope, thereby accomplishing a suitable UV coverage in application to multi-aperture interferometers.

A. Rotational Phase Synchronization for Spacecraft Positions

This section extends the phase synchronization of a single variable from Ref. 32 to Lagrangian systems of multiple degrees-of-freedom on a two-dimensional plane with the proposed control law that has a hierarchical structure. A new proof for phase synchronization is presented such that the angular transformation terms in the Laplacian matrix disappear. By combining the trajectory control with the synchronization coupling, we can achieve much more efficient and robust performance that is essential to precision formation flight of spacecraft.

For the relative translational dynamics presented in (12), the following decentralized tracking control law with two-way-ring symmetry is proposed for the i-th spacecraft in the circular network comprised of p *identical* spacecraft ($1 \leq i \leq p$):

$$\mathbf{F}_i = \mathbf{M}\ddot{\mathbf{r}}_{r,i} + \mathbf{C}\dot{\mathbf{r}}_{r,i} + \mathbf{D}(\mathbf{r}_i)\mathbf{r}_i + \mathbf{g}(\mathbf{r}_i) - k_1\mathbf{s}_i^{\text{pos}} + k_2\mathbf{T}(\theta)\mathbf{s}_{i-1}^{\text{pos}} + k_2\mathbf{T}^T(\theta)\mathbf{s}_{i+1}^{\text{pos}} \tag{37}$$

where k_1 and k_2 are positive constants, and the rotation matrix $\mathbf{T}(\theta) \in \mathcal{SO}(2)$ is defined as

$$\mathbf{T}(\theta) = \begin{bmatrix} \cos\theta & 0 & -\sin\theta \\ 0 & 1 & 0 \\ \sin\theta & 0 & \cos\theta \end{bmatrix} \tag{38}$$

Note that $\mathbf{T}^T(\theta) = \mathbf{T}^{-1}(\theta) = \mathbf{T}(-\theta)$ and $\mathbf{T}(p\theta) = \mathbf{I}$ since $\theta = 2\pi/p$.

For two-spacecraft networks, the last coupling term with the $(i+1)$-th member is not used. Also, the shifted reference velocity vector $\dot{\mathbf{r}}_{r,i}$ and the composite variable $\mathbf{s}_i^{\text{pos}}$ are defined as follows:

$$\dot{\mathbf{r}}_{r,i} = \dot{\mathbf{r}}_{d,i} + \lambda(\mathbf{r}_{d,i} - \mathbf{r}_i), \quad \mathbf{s}_i^{\text{pos}} = \dot{\mathbf{r}}_i - \dot{\mathbf{r}}_{r,i} = \dot{\mathbf{r}}_i - \dot{\mathbf{r}}_{d,i} + \lambda(\mathbf{r}_i - \mathbf{r}_{d,i}) \tag{39}$$

where λ is a positive constant. The time-varying desired trajectory $\mathbf{r}_{d,i}$ is different for each spacecraft since its phase is shifted from its neighbors by $\pm\theta$:

$$\begin{aligned}
\mathbf{r}_{d,1} &= \Big(a(t)\cos\omega t, \quad y_d(t), \quad a(t)\sin\omega t\Big)^T = \mathbf{r}_d \\
\mathbf{r}_{d,2} &= \Big(a(t)\cos[\omega t + \theta], \quad y_d(t), \quad a(t)\sin[\omega t + \theta]\Big)^T = \mathbf{T}(\theta)\mathbf{r}_d \\
&\vdots \\
\mathbf{r}_{d,i} &= \Big(a(t)\cos[\omega t + (i-1)\theta], \quad y_d(t), \quad a(t)\sin[\omega t + (i-1)\theta]\Big)^T = \mathbf{T}((i-1)\theta)\mathbf{r}_d
\end{aligned} \tag{40}$$

Note that, in a 2-dimensional circular trajectory orthogonal to the orbital plane, the radius $a(t)$ becomes a constant and y_d reduces to zero.

The closed-loop dynamics for the i-th satellite, constructed from (12) and (37), becomes

$$\mathbf{M}\dot{\mathbf{s}}_i^{\text{pos}} + \mathbf{C}\mathbf{s}_i^{\text{pos}} + k_1\mathbf{s}_i^{\text{pos}} - k_2\mathbf{T}(\theta)\mathbf{s}_{i-1}^{\text{pos}} - k_2\mathbf{T}^T(\theta)\mathbf{s}_{i+1}^{\text{pos}} = \mathbf{0} \tag{41}$$

By inspecting Figure 3, we can find the new flow-invariant set of $\mathbf{s}_i^{\text{pos}}$ that is phase-shifted from the original invariant set $\mathbf{s}_1^{\text{pos}} = \mathbf{s}_2^{\text{pos}} = \cdots = \mathbf{s}_p^{\text{pos}}$:

$$\mathbf{s}_1^{\text{pos}} \quad = \quad \mathbf{T}^T(\theta)\mathbf{s}_2^{\text{pos}} \quad = \quad \cdots \quad = \quad \mathbf{T}^T((p-1)\theta)\mathbf{s}_p^{\text{pos}} \tag{42}$$

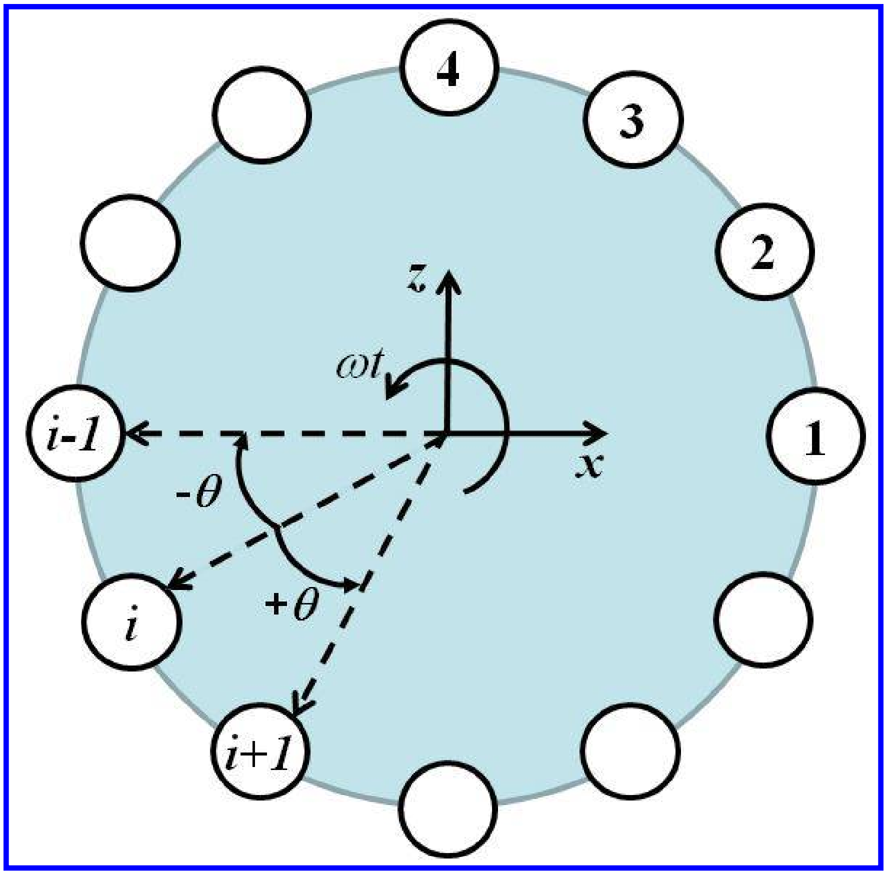

Figure 3. Geometry of a circular rotating trajectory. The x-z axes denote F^{RO} in Figure 1.

where the matrix of the orthonormal eigenvectors $\mathbf{V}$ is obtained from (27).

Left-multiplying (41) with $\mathbf{T}^T((i-1)\theta)$ for each spacecraft results in

$$[\mathbf{M}^{\text{pos}}]\dot{\mathbf{x}}^{\text{pos}} + [\mathbf{C}^{\text{pos}}]\mathbf{x}^{\text{pos}} + [\mathbf{L}^p_{\mathbf{K}_1,-\mathbf{K}_2}]\mathbf{x}^{\text{pos}} = \mathbf{0} \tag{43}$$

where

$$[\mathbf{M}^{\text{pos}}] = \begin{bmatrix} \mathbf{M}_{T,1} & \cdots & \mathbf{0} \\ \vdots & \ddots & \vdots \\ \mathbf{0} & \cdots & \mathbf{M}_{T,p} \end{bmatrix}, \quad [\mathbf{C}^{\text{pos}}] = \begin{bmatrix} \mathbf{C}_{T,1} & \cdots & \mathbf{0} \\ \vdots & \ddots & \vdots \\ \mathbf{0} & \cdots & \mathbf{C}_{T,p} \end{bmatrix}, \quad \mathbf{x}^{\text{pos}} = \begin{pmatrix} \mathbf{s}^{\text{pos}}_1 \\ \vdots \\ \mathbf{T}^T((p-1)\theta)\mathbf{s}^{\text{pos}}_p \end{pmatrix} \tag{44}$$

Also, $\mathbf{M}_{T,i} = \mathbf{T}^T((i-1)\theta)\mathbf{M}\mathbf{T}((i-1)\theta) = \mathbf{M}$ and $\mathbf{C}_{T,i} = \mathbf{T}^T((i-1)\theta)\mathbf{C}\mathbf{T}((i-1)\theta)$ where the $\mathbf{M}$ and $\mathbf{C}$ matrices are defined in (12). Hence, $\dot{\mathbf{M}}_{T,i} - 2\mathbf{C}_{T,i} = -2\mathbf{C}_{T,i}$ is skew-symmetric. Then, similar to the previous section, we can prove the synchronization $\mathbf{V}^T_{sync}\mathbf{x}^{\text{pos}} \to \mathbf{0}$ as well as the tracking convergence $\mathbf{s}^{\text{pos}}_i \to \mathbf{0}$ by constructing the virtual system and performing the spectral decomposition as follows:

$$\left(\mathbf{V}^T[\mathbf{M}^{\text{pos}}]\mathbf{V}\right)\dot{\mathbf{y}} + \left(\mathbf{V}^T[\mathbf{C}^{\text{pos}}]\mathbf{V}\right)\mathbf{y} + [\mathbf{D}]\mathbf{y} = \mathbf{0} \tag{45}$$

Note that (45) has $\mathbf{y} = \mathbf{V}^T\mathbf{x}^{\text{pos}} = ([\mathbf{1}], \mathbf{V}_{sync})^T\mathbf{x}^{\text{pos}}$ and $\mathbf{y} = \mathbf{0}$ as particular solutions. Due to the skew-symmetry of $\mathbf{C}$, (45) is contracting with $[\mathbf{D}] > 0$, resulting in the tracking stability $\mathbf{s}^{\text{pos}}_i \to 0$ as well as

$$\mathbf{s}^{\text{pos}}_1 \leftrightarrow \mathbf{T}^T(\theta)\mathbf{s}^{\text{pos}}_2 \leftrightarrow \mathbf{T}^T((i-1)\theta)\mathbf{s}^{\text{pos}}_i \leftrightarrow \mathbf{T}^T((p-1)\theta)\mathbf{s}^{\text{pos}}_p \tag{46}$$

From the hierarchical combination of the composite variable and the definition of $\mathbf{r}_{d,i}$, one can verify that

$$\begin{aligned} \dot{\mathbf{r}}_i + \lambda\mathbf{r}_i + \mathbf{T}((i-1)\theta)(\dot{\mathbf{r}}_d + \lambda\mathbf{r}_d) &= \mathbf{s}^{\text{pos}}_i \\ \dot{\mathbf{r}}_{i+1} + \lambda\mathbf{r}_{i+1} + \mathbf{T}(i\theta)(\dot{\mathbf{r}}_d + \lambda\mathbf{r}_d) &= \mathbf{s}^{\text{pos}}_{i+1} \end{aligned} \tag{47}$$

Left-multiplying the dynamic equation of $\mathbf{r}_i$ in (47) with $\mathbf{T}^T((i-1)\theta)$, and that of of $\mathbf{r}_{i+1}$ with $\mathbf{T}^T((i)\theta)$ result in

$$\begin{aligned}\mathbf{T}^T((i-1)\theta)\dot{\mathbf{r}}_i + \lambda\mathbf{T}^T((i-1)\theta)\mathbf{r}_i = u(t)\\ \mathbf{T}^T(i\theta)\dot{\mathbf{r}}_{i+1} + \lambda\mathbf{T}^T(i\theta)\mathbf{r}_{i+1} = u(t)\end{aligned} \tag{48}$$

where the common input verifies $u(t) = -(\dot{\mathbf{r}}_d + \lambda\mathbf{r}_d)$ if the phase-shifted composite variables synchronize, that is $\mathbf{T}^T((i-1)\theta)\mathbf{s}_i^{\text{pos}} = \mathbf{T}^T(i\theta)\mathbf{s}_{i+1}^{\text{pos}}$.

From (48), $\lambda > 0$ ensures that $\mathbf{T}^T((i-1)\theta)\mathbf{r}_i$ exponentially tends to $\mathbf{T}^T(i\theta)\mathbf{r}_{i+1}$ since $\dot{\mathbf{y}} + \lambda\mathbf{y} = 0$ is contracting (Theorem VI.1 and Theorem VI.4). This concludes the proof of the phase synchronization of the relative translational dynamics for the case of multiple identical spacecraft on a circular or spiral trajectory. For heterogeneous spacecraft, we can scale the control gains k_1 and k_2 according to the mass ratio, and the proof essentially remains the same.

B. Synchronized Rotational Maneuvers

One can easily construct the combined dynamics of both attitude rotation and relative position as follows

$$\begin{bmatrix}[\mathbf{M}] & 0\\ 0 & [\mathbf{M}^{pos}]\end{bmatrix}\begin{pmatrix}\ddot{\mathbf{x}}\\ \ddot{\mathbf{x}}^{pos}\end{pmatrix} + \begin{bmatrix}[\mathbf{C}] & 0\\ 0 & [\mathbf{C}^{pos}]\end{bmatrix}\begin{pmatrix}\dot{\mathbf{x}}\\ \dot{\mathbf{x}}^{pos}\end{pmatrix} + \begin{bmatrix}[\mathbf{L}^p_{\mathbf{K}_1,-\mathbf{K}_2}] & 0\\ 0 & [\mathbf{L}^p_{\mathbf{K}_1,-\mathbf{K}_2}]\end{bmatrix}\begin{pmatrix}\mathbf{x}\\ \mathbf{x}^{pos}\end{pmatrix} = \mathbf{0} \tag{49}$$

where we used the control law (14) for the rotational attitude dynamics and the control law (37) for the translational dynamics.

We can also demonstrate the synchronized rotation maneuver[14] by synchronizing the desired rotational rate of the attitude dynamics from $\mathbf{q}_d(t)$ and $\dot{\mathbf{q}}_d(t)$ with the rotational rate ω of the desired circular trajectory $\mathbf{r}_d$ defined in (40).

V. Extensions and Examples

Let us examine the effectiveness of the proposed control law in a few examples.

A. Effects of External Disturbances

Equation (31), in the presence of the external disturbance torque $\tau_{\mathbf{ext}}$, can be written as

$$\left(\mathbf{V}^T[\mathbf{M}]\mathbf{V}\right)\begin{pmatrix}[\mathbf{1}]^T\dot{\mathbf{x}}\\ \mathbf{V}^T_{sync}\dot{\mathbf{x}}\end{pmatrix} + \left(\mathbf{V}^T[\mathbf{C}]\mathbf{V} + [\mathbf{D}]\right)\begin{pmatrix}[\mathbf{1}]^T\mathbf{x}\\ \mathbf{V}^T_{sync}\mathbf{x}\end{pmatrix} = \begin{pmatrix}[\mathbf{1}]^T\\ \mathbf{V}^T_{sync}\end{pmatrix}\begin{pmatrix}\tau_{\mathbf{ext,1}}\\ \vdots\\ \tau_{\mathbf{ext,p}}\end{pmatrix} \tag{50}$$

which indicates that the disturbance input for the synchronization is only the difference among each disturbance force/torque $\mathbf{V}^T_{sync}(\tau_{\mathbf{ext,1}}{}^T, \cdots, \tau_{\mathbf{ext,p}}{}^T)^T$. As a result, the disturbance torque that is invariant from spacecraft to spacecraft, does not affect the synchronization of the relative attitude, which might be of more importance than the performance of trajectory following. For example, stellar interferometers need precise control of relative attitude and distance between spacecraft that carry telescopes.

Now we consider the bounded vanishing disturbance of the individual tracking dynamics. Due to exponential tracking convergence of the proposed scheme, the property of robustness to bounded deterministic disturbances can easily be determined. For example, consider the closed-loop system in (19), which is now subject to a vanishing perturbation[19] such that $\mathbf{d}(t, \mathbf{x} = \mathbf{0}) = \mathbf{0}$:

$$[\mathbf{M}]\dot{\mathbf{x}} + [\mathbf{C}]\mathbf{x} + [\mathbf{L}^p_{\mathbf{K}_1,-\mathbf{K}_2}]\mathbf{x} = \mathbf{d}(t, \mathbf{x}) \tag{51}$$

The perturbation term $\mathbf{d}(t, \mathbf{x})$ vanishes at the equilibrium manifold $\mathbf{x} = \mathbf{0}$. Let us further assume that it satisfies the linear growth bound such that

$$\|\mathbf{d}(t, \mathbf{x})\| \leq \gamma\|\mathbf{x}\|, \quad \forall t > 0. \tag{52}$$

where γ is a positive constant.

The squared-length analysis yields

$$
\begin{aligned}
\frac{d}{dt}\left(\delta\mathbf{x}^T[\mathbf{M}]\delta\mathbf{x}\right) &= 2\delta\mathbf{x}^T[\mathbf{M}]\delta\dot{\mathbf{x}} + \delta\mathbf{x}^T[\dot{\mathbf{M}}]\delta\mathbf{x} \\
&= 2\delta\mathbf{x}^T\left(-[\mathbf{C}]\delta\mathbf{x} - [\mathbf{L}^p_{\mathbf{K}_1,-\mathbf{K}_2}]\delta\mathbf{x} + \delta\mathbf{d}(t,\mathbf{x})\right) + \delta\mathbf{x}^T[\dot{\mathbf{M}}]\delta\mathbf{x} \\
&\leq -2\delta\mathbf{x}^T\left([\mathbf{L}^p_{\mathbf{K}_1,-\mathbf{K}_2}] - \gamma\mathbf{I}\right)\delta\mathbf{x}
\end{aligned}
\tag{53}
$$

where we used the skew-symmetric property of $[\dot{\mathbf{M}}] - 2[\mathbf{C}]$.

Hence, the closed-loop system in (51) is contracting in the presence of the bounded disturbance if $[\mathbf{L}^p_{\mathbf{K}_1,-\mathbf{K}_2}] > \gamma\mathbf{I}$. As a result, the trajectory tracking gain (slower gain) also determines how robust the closed-loop system is with respect to a bounded disturbance.

For a nonvanishing perturbation such that

$$
\|\mathbf{d}(t,\mathbf{x})\| \leq \gamma\|\mathbf{x}\| + \Delta \tag{54}
$$

where Δ is bounded, the comparison method[19] can straightforwardly be developed to derive a bound on the solution. Alternatively, we can follow the analysis of contraction with respect to a property of robustness.[21,32]

We assume that $P_1(t)$ represents a desired system trajectory and $P_2(t)$ the actual system trajectory in a disturbed flow field given in (51). Also, consider the distance $R(t)$ between two trajectories $P_1(t)$ and $P_2(t)$ such that

$$
R(t) = \int_{P_1}^{P_2} \|\delta\mathbf{z}\| = \int_{P_1}^{P_2} \|\mathbf{\Theta}(\mathbf{x})\delta\mathbf{x}\| \tag{55}
$$

where $\mathbf{\Theta}(\mathbf{x})^T\mathbf{\Theta}(\mathbf{x}) = [\mathbf{M}]$ (see the Appendix).

Then, by combining the results from (53), (54), and Ref. 21, we can show that any trajectory converges exponentially to a ball of radius of R around the desired trajectory such that

$$
R(t) \leq \sup_{\mathbf{x},t}\|\mathbf{\Theta}(\mathbf{x})^{-T}\Delta\|/\lambda_{max} \tag{56}
$$

where the contraction rate λ_{max}, in the context of contraction theory, is defined with respect to $\delta\mathbf{z} = \mathbf{\Theta}(\mathbf{x})\delta\mathbf{x}$, and is given by $[\mathbf{M}]^{-1}\left([\mathbf{L}^p_{\mathbf{K}_1,-\mathbf{K}_2}] - \gamma\mathbf{I}\right)$ from (53). It should be emphasized that the exponential stability of the closed-loop system facilitates such a perturbation analysis, which showcases another benefit of contraction analysis. In contrast, the proof of robustness with asymptotic convergence is more involved.[19]

B. Attitude Synchronization of Two Spacecraft

The proposed control law in (14) is simulated for two identical spacecraft, as shown in Figure 4(a). The spacecraft inertial matrix is

$$
\mathbf{J_{s/c}} = \begin{bmatrix} 150 & 0 & -100 \\ 0 & 270 & 0 \\ -100 & 0 & 300 \end{bmatrix} \quad [\text{kgm}^2] \tag{57}
$$

The control gains are defined as $\mathbf{K}_1 = 300\mathbf{I}$, $\mathbf{K}_2 = 100\mathbf{I}$, and $\mathbf{\Lambda} = 20\mathbf{I}$. The reference trajectories are defined as $\mathbf{q}_{1d} = 0.3\sin(2\pi(0.01)t)$, $\mathbf{q}_{2d} = 0.2\sin(2\pi(0.02)t + \pi/6)$, and $\mathbf{q}_{3d} = 0$. The first spacecraft is initially at $(0.05, -0.1, 0)^T$ rad, with zero angular rates, while all the initial conditions for the second spacecraft are zero.

The synchronization gain of $\mathbf{s}_1$ and $\mathbf{s}_2$ corresponds to $\mathbf{K}_1 + \mathbf{K}_2 = 400\mathbf{I}$, which is larger than the tracking convergence gain $\mathbf{K}_1 - \mathbf{K}_2 = 200\mathbf{I}$. As a result, we can see , in Figure 4, that the first and second spacecraft exponentially synchronize first. Then, they exponentially converge together to the desired trajectory.

In order to compare the effectiveness of the exponential tracking, a simple Proportional and Derivative (PD) diffusive coupling, introduced in Ref. 4, 17, is simulated for the comparison purpose, as shown in Figure 4(b). The control law for two spacecraft can be given as

$$
\begin{aligned}
\tau_1 &= -\mathbf{K}_1(\dot{\mathbf{q}}_1 + \mathbf{\Lambda}\tilde{\mathbf{q}}_1) + \mathbf{K}_2(\dot{\mathbf{q}}_2 + \mathbf{\Lambda}\tilde{\mathbf{q}}_2) \\
\tau_2 &= -\mathbf{K}_1(\dot{\mathbf{q}}_2 + \mathbf{\Lambda}\tilde{\mathbf{q}}_2) + \mathbf{K}_2(\dot{\mathbf{q}}_1 + \mathbf{\Lambda}\tilde{\mathbf{q}}_1)
\end{aligned}
\tag{58}
$$

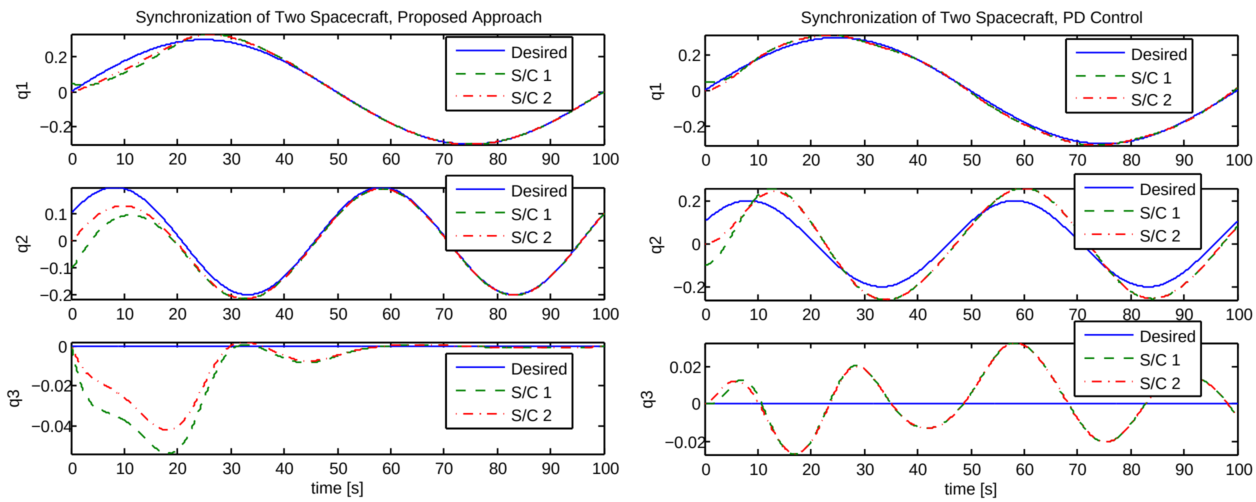

(a) Proposed control law

(b) Simple PD diffusive coupling

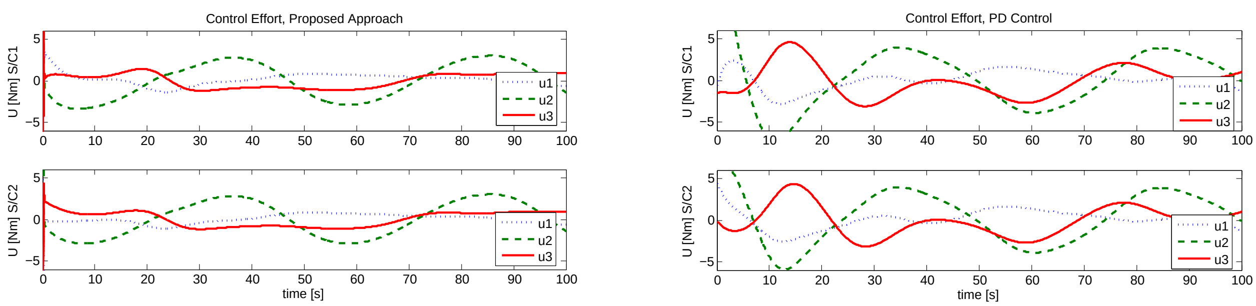

(c) Control effort: proposed control

(d) Control effort: PD control

Figure 4. Synchronization of the attitude dynamics of two identical spacecraft

whose global asymptotic stability with respect to a constant reference input is proven in Ref. 4, 17. For a fair comparison, we selected the PD gains in (58) as $\mathbf{K}_1 = 1000$, $\mathbf{K}_2 = 300$, and $\mathbf{\Lambda} = 0.3$ such that the level of control efforts is comparable to that of nonlinear control approach in (14). As shown in Figure 4(b), the PD coupling control law is not effective in following a time-varying trajectory. This is because simple linear control cannot be expected to handle the dynamic demands of efficiently following time-varying trajectories. Specifically, achieving exponential convergence ensures more effective tracking performance than asymptotic convergence by linear PD control. Even if the torque actuators saturate at 6 Nm, the results do not change.

C. Position and Attitude Synchronization of Two Spacecraft Under J2 Effect

A full 6 DOF simulation of a two identical satellite formation using the proposed phase synchronization control law (37) and with the attitude tracking (2) was prepared. Full nonlinear attitude and translational dynamics including J2 effect were simulated for each satellite in the formation. The mass of each satellite is assumed to be 500 kg. The spacecraft inertia matrix is given from the two-spacecraft example in Ref. 6. The attitude control gains were defined as $\mathbf{K}_1 = 30\mathbf{I}$, $\mathbf{K}_2 = 20\mathbf{I}$ and $\mathbf{\Lambda} = 20\mathbf{I}$. The attitude reference trajectories were defined to be $q_{1d} = 0.3\sin(2\pi \times 0.001t)$, $q_{2d} = 0.2\sin(2\pi \times 0.002t + \pi/6)$, and $q_{3d} = 0$, which are similar (but at a lower frequency) to the previous example.

For the translational control the gains were defined to be same for both the satellites as $k_1 = 10$, $k_2 = 5$ and $\lambda = 2$. The desired trajectory for the formation was defined so that the satellites would follow a spiral trajectory such that both satellites maintain a phase angle of 180 deg. The desired spiral trajectory was defined as $\mathbf{r}_d = [a(t)\sin\omega t, 0, a(t)\cos\omega t]^T$ from (40), where $a(t) = 5+0.0001t$ and $\omega = 2\pi/500$ (see the actual plot of this spiral trajectory generated from the actual simulation in Fig. 5). The formation was placed in a polar circular orbit at an altitude of 500 km and it was subject to J2 perturbations in the nonlinear model. Figure 6 shows the robust synchronization performance in the presence of non-identical disturbance such as

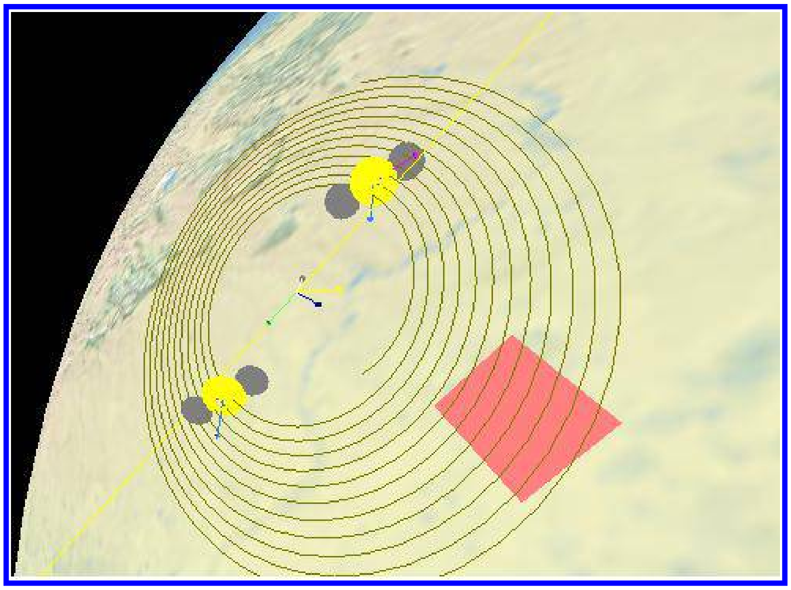

Figure 5. Three-dimensional simulation of the phase synchronization on a spiral trajectory

the differential J2 effect. It should be noted that this scheme requires information from only the adjacent spacecraft, thus this scheme is suitable for implementing a distributed control architecture.

VI. Conclusions

We have introduced the new unified synchronization framework that integrates both the exponential tracking of a demanding time-varying trajectory and the synchronization of spacecraft motions either through local coupling feedback or a relative sensing metrology system. The new decentralized control laws, developed by utilizing the Lagrangian formulations of the translational dynamics and attitude dynamics of spacecraft, enable coupled rotational maneuvers and phase synchronization of the attitude and position, thereby facilitating a further analysis on stability, adaptation, and robustness. In order to rigorously address the three main areas of research for the realization of future spacecraft formation flying missions, we have focused on the three research areas: (1) the exact nonlinear stability conditions of multiple spacecraft dynamics, (2) the reduced information networks through local interactions, and (3) the properties of robustness with respect to uncertain models. In particular, in contrast with prior work which used simple single or double integrator models, the proposed method is applicable to highly nonlinear systems with nonlinearly coupled inertia matrices such as the attitude dynamics of spacecraft. It should be noted again that one of the main contributions of this paper lies with the use of a new differential nonlinear stability framework called contraction theory, yielding the exact proof of nonlinear stability under a variety of conditions, while others can still come up with nonlinear control laws, similar to our approach, without a rigorous stability proof. Contraction analysis, overcoming a local result of Lyapunov's indirect method, yields global results based on differential stability analysis. The benefit of constructing multiple timescales of the closed-loop system is that exponential synchronization, with a convergence rate faster than that of the trajectory tracking, enables reduction of multiple dynamics into a simpler synchronized form, thereby simplifying the additional stability analysis. We illustrated the effectiveness of the proposed approach by simulating the combined rotational and translational maneuvers in the presence of variation in the second-degree zonal harmonic J2 of the Earth's gravitational potential.

ACKNOWLEDGMENTS

This work has benefitted from stimulating discussions with Dr. David W. Miller at MIT, Dr. Bong Wie at Iowa State University, and Dr. Jesse Leitner at the NASA Goddard Space Flight Center. The authors

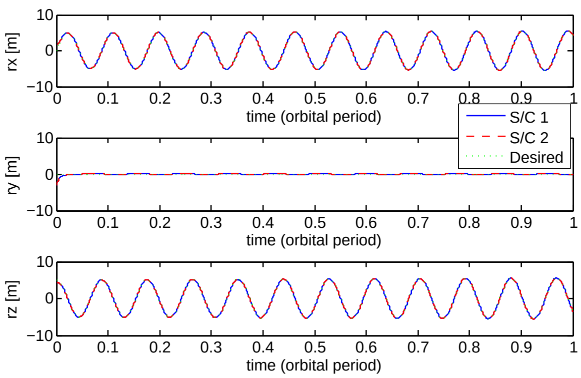

(a) Results of the simulation for two spacecraft phase synchronization

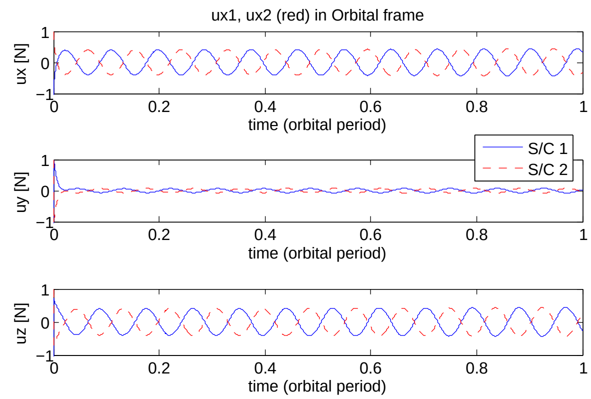

(b) Control forces

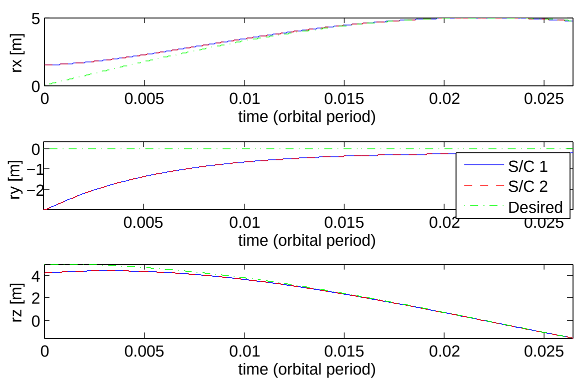

(c) Initial synchronization of the formation with the desired trajectory.

Figure 6. Simulation of the proposed control law for the combined translational and rotational dynamics.

would like to acknowledge the constructive feedback from anonymous reviewers.

APPENDIX: Contraction Theory

We exploit partial contraction theory[23] to prove the stability of coupled nonlinear dynamics. Lyapunov's linearization method indicates that the local stability of the nonlinear system can be analyzed using its differential approximation. What is new in contraction theory is that a differential stability analysis can be made exact, thereby yielding global results on the nonlinear system. A brief review of the results from[21–23] is presented in this section. Readers are referred to these references for detailed descriptions and proofs on the following theorems. Note that contraction theory is a generalization of the classical Krasovskii's theorem.[18]

Consider a smooth nonlinear system

$$\dot{\mathbf{x}}(t) = \mathbf{f}(\mathbf{x}(t), \mathbf{u}(\mathbf{x}, t), t) \tag{59}$$

where $\mathbf{x}(t) \in \mathbb{R}^n$, and $\mathbf{f} : \mathbb{R}^n \times \mathbb{R}^m \times \mathbb{R}_+ \to \mathbb{R}^n$. A virtual displacement, $\delta\mathbf{x}$ is defined as an infinitesimal displacement at a fixed time– a common supposition in the calculus of variations.

Theorem VI.1 *For the system in (59), if there exists a uniformly positive definite metric,*

$$\mathbf{M}(\mathbf{x}, t) = \mathbf{\Theta}(\mathbf{x}, t)^T \mathbf{\Theta}(\mathbf{x}, t) \tag{60}$$

where $\mathbf{\Theta}$ is some smooth coordinate transformation of the virtual displacement, $\delta\mathbf{z} = \mathbf{\Theta}\delta\mathbf{x}$, such that the associated generalized Jacobian, $\mathbf{F}$ is uniformly negative definite, i.e., $\exists\lambda > 0$ such that

$$\mathbf{F} = \left(\dot{\mathbf{\Theta}}(\mathbf{x}, t) + \mathbf{\Theta}(\mathbf{x}, t)\frac{\partial \mathbf{f}}{\partial \mathbf{x}}\right)\mathbf{\Theta}(\mathbf{x}, t)^{-1} \leq -\lambda\mathbf{I}, \tag{61}$$

then all system trajectories converge globally to a single trajectory exponentially fast regardless of the initial conditions, with a global exponential convergence rate of the largest eigenvalues of the symmetric part of $\mathbf{F}$.

Such a system is said to be contracting. The proof is given in Ref. 21. Equivalently, the system is contracting if $\exists\lambda > 0$ such that

$$\dot{\mathbf{M}} + \left(\frac{\partial \mathbf{f}}{\partial \mathbf{x}}\right)^T \mathbf{M} + \mathbf{M}\frac{\partial \mathbf{f}}{\partial \mathbf{x}} \leq -2\lambda\mathbf{M} \tag{62}$$

It can also be shown that for a contracting autonomous system of the form $\dot{\mathbf{x}} = \mathbf{f}(\mathbf{x}, \mathbf{u}(\mathbf{x}))$, all trajectories converge to an equilibrium point exponentially fast. In essence, contraction analysis implies that stability of nonlinear systems can be analyzed more simply by checking the negative definiteness of a proper matrix, rather than finding some implicit motion integral as in Lyapunov theory.

The following theorems are used to derive stability and synchronization of the coupled dynamics systems.

Theorem VI.2 ***Hierarchical combination***[22, 23]
Consider two contracting systems, of possibly different dimensions and metrics, and connect them in series, leading to a smooth virtual dynamics of the form

$$\frac{d}{dt}\begin{pmatrix}\delta\mathbf{z_1}\\ \delta\mathbf{z_2}\end{pmatrix} = \begin{pmatrix}\mathbf{F_{11}} & \mathbf{0}\\ \mathbf{F_{21}} & \mathbf{F_{22}}\end{pmatrix}\begin{pmatrix}\delta\mathbf{z_1}\\ \delta\mathbf{z_2}\end{pmatrix}$$

Then the combined system is contracting if $\mathbf{F_{21}}$ is bounded.

Theorem VI.3 ***Partial contraction***[23]
Consider a nonlinear system of the form $\dot{\mathbf{x}} = \mathbf{f}(\mathbf{x}, \mathbf{x}, t)$ and assume that the auxiliary system $\dot{\mathbf{y}} = \mathbf{f}(\mathbf{y}, \mathbf{x}, t)$ is contracting with respect to $\mathbf{y}$. If a particular solution of the auxiliary $\mathbf{y}$-system verifies a specific smooth property, then all trajectories of the original x-system verify this property exponentially. The original system is said to be partially contracting.

Theorem VI.4 ***Synchronization***[23]
Consider two coupled systems. If the dynamics equations verify

$$\dot{\mathbf{x}}_1 - \mathbf{f}(\mathbf{x}_1, t) = \dot{\mathbf{x}}_2 - \mathbf{f}(\mathbf{x}_2, t)$$

where the function $\mathbf{f}(\mathbf{x}, t)$ is contracting in an input-independent metric, then $\mathbf{x}_1$ and $\mathbf{x}_2$ will converge to each other exponentially, regardless of the initial conditions. Mathematically, stable concurrent synchronization corresponds to convergence to a flow-invariant linear subspace of the global state space.[32]

References

[1]Leitner, J., Carpenter, J. R., Naasz, B. J., Ahmed, A., Hadaegh, F. Y., and Scharf, D. P., "A Concept for In-space, System-level Validation of Spacecraft Precision Formation Flying," Proceedings of the AIAA Guidance, Navigation and Control Conference and Exhibit, AIAA Paper 2007-6541, Hilton Head, SC, Aug. 2007.

[2]Chung, S.-J., Slotine, J.-J. E., and Miller, D. W., "Nonlinear Model Reduction and Decentralized Control of Tethered Formation Flight," *Journal of Guidance, Control, and Dynamics*, Vol. 30, No. 2, 2007, pp. 390–400.

[3]Ahsun, U., "Dynamics and Control of Electromagnetic Satellite Formations," Ph.D. Thesis, Dept. of Aeronautics and Astronautics, Massachusetts Inst. of Technology, Cambridge, MA, 2007, http://dspace.mit.edu.

[4]Chung, S.-J., *Nonlinear Control and Synchronization of Multiple Lagrangian Systems with Application to Tethered Formation Flight Spacecraft*, Sc.D. Thesis, Dept. of Aeronautics and Astronautics, Massachusetts Inst. of Technology, Cambridge, MA, 2007, http://dspace.mit.edu.

[5]Chung, S.-J., Miller, D. W., deWeck, O. L., "ARGOS Testbed: Study of Multidisciplinary Challenges of Future Spaceborne Interferometric Arrays," *Optical Engineering*, Vol. 43, No. 9, September 2004, pp. 2156–2167.

[6]Chung, S.-J., Umair, A., and Slotine, J.-J.E.,"Application of Synchronization to Cooperative Control and Formation Flight of Spacecraft," Proceedings of the AIAA Guidance, Navigation and Control Conference, Hilton Head, SC, 2007, AIAA-2007-6861.

[7]Scharf, D. P., Hadaegh, F. Y., and Ploen, S. R., "A Survey of Spacecraft Formation Flying Guidance and Control (Part I): Guidance," Proceedings of the American Control Conference, Denver, CO, June 4–6, 2003, pp. 1733–1739.

[8]Scharf, D. P., Hadaegh, F. Y., and Ploen, S. R., "A Survey of Spacecraft Formation Flying Guidance and Control (Part II): Control," Proceedings of the American Control Conference, Denver, CO, June 4–6, 2003, pp. 2976–2985.

[9]Olfati-Saber, R., and Murray, R. M., "Consensus Problems in Networks of Agents with Switching Topology and Time-Delays," *IEEE Transactions On Automatic Control*, Vol. 49, No. 9, Sept. 2004, pp. 1520–1533.

[10]Olfati-Saber, R., "Flocking for Multi-Agent Dynamic Systems: Algorithms and Theory," *IEEE Transactions on Automatic Control*, Vol. 51, No. 3, 2006, pp. 401-420.

[11]Jadbabaie, A., Lin, J., and Morse, A. S., "Coordination of Groups of Mobile Autonomous Agents Using Nearest Neighbor Rules," *IEEE Transactions on Automatic Control*, Vol. 48, No. 6, June 2003, pp. 988–1001.

[12]Mesbahi, M., and Hadaegh, F. Y., "Formation Flying of Multiple Spacecraft via Graphs, Matrix Inequalities, and Switching," *Journal of Guidance, Control, and Dynamics*, Vo. 24, No. 2, 2001, pp. 369–377.

[13]Pan, H., and Kapila, V.,"Adaptive Nonlinear Control for Spacecraft Formation Flying with Coupled Translational and Attitude Dynamics," Proc. of the 40th IEEE Conference on Decision and Control, Orlando, FL, Vol. 3, December 2001, pp. 2057–2062.

[14]Wang, P. K. C., Hadaegh, F. Y., and Lau, K., "Synchronized Formation Rotation and Attitude Control of Multiple Free-Flying Spacecraft," *Journal of Guidance, Control, and Dynamics*, Vol. 22, No. 1, 1999, pp. 28–35.

[15]Lawton, J., and Beard, R. W., "Synchronized Multiple Spacecraft Rotations," *Automatica*, Vol. 38, No. 8, 2002. pp. 1359-1364.

[16]Ren, W., "Formation Keeping and Attitude Alignment for Multiple Spacecraft through Local Interactions," *Journal of Guidance, Control and Dynamics*, Vol. 30, No. 2, March-April 2007, pp. 633-638.

[17]Chung, S.-J., and Slotine, J.-J. E, "Cooperative Robot Control and Concurrent Synchronization of Lagrangian Systems," *IEEE Transactions on Robotics*, in review, 2008.

[18]Slotine, J.-J. E., and Li, W., *Applied Nonlinear Control*, Prentice Hall, Upper Saddle River, NJ, 1991, pp. 41–154.

[19]Khalil, H. K., *Nonlinear Systems*, 3rd ed., Prentice Hall, Upper Saddle River, NJ, 2002, pp. 339–372.

[20]Wie, B., *Space Vehicle Dynamics and Control*, AIAA, Reston, Virginia, pp. 435–445.

[21]Lohmiller, W., and Slotine, J.J.E., "On Contraction Analysis for Nonlinear Systems," *Automatica*, Vol. 34, No. 6, 1998, pp. 683-696.

[22]Slotine, J.-J. E., "Modular Stability Tools for Distributed Computation and Control," *Intertnational Journal of Adaptive Control and Signal Processing*, vo. 17, no. 6, 2003, pp. 397–416.

[23]Wang, W., and Slotine, J.J.E., "On Partial Contraction Analysis for Coupled Nonlinear Oscillators," *Biological Cybernetics*, Vol. 92, No. 1, 2004, pp. 38-53.

[24]Wang, W., and Slotine, J.-J. E., "Contraction Analysis of Time-Delayed Communications Using Simplified Wave Variables," *IEEE Transactions on Automatic Control*, Vol. 51, No. 5, 2006, pp. 712–717.

[25]Vadali, S. R., Vaddi, S. S., Naik, K., and Alfriend, K. T., "Control of Satellite Formations," AIAA Guidance, Navigation, and Control Conference and Exhibit, AIAA Paper 2001-4028, 6-9 August, 2001.

[26]Kasdin, N.J., Gurfil, P., and Kolemen, E., "Canonical Modeling of Relative Spacecraft Motion via Epicyclic Orbital Elements", *Celestial Mechanics and Dynamical Astronomy*, Vol. 92, No. 4, 2005, pp. 337-370.

[27]Breger, L, and How, J. P., "Gauss's Variational Equation-Based Dynamics and Control for Formation Flying Spacecraft," *Journal of Guidance, Control, and Dynamics*, Vol. 30, No. 2, pp. 437-448, 2007.

[28]Slotine, J.-J. E. and Benedetto, M. D. D., "Hamiltonian Adaptive Control of Spacecraft," *IEEE Transactions on Automatic Control*, Vol. 35, No. 7, July 1990, pp. 848-852. doi:10.1109/9.57028

[29]Yoon, H., and Tsiotras, P., "Spacecraft Adaptive Attitude and Power Tracking with Variable Speed Control Moment Gyroscopes," *Journal of Guidance, Control, and Dynamics*, Vol. 25, No. 6, pp. 1081–1090, November-December 2002.

[30]Shuster, M.D., "A Survey of Attitude Representations," *Journal of the Astronautical Sciences*, Vol. 41, No. 4, pp. 439–517, 1993.

[31]Schaub, H., and Junkins, J. L, "Stereographic Orientation Parameters for Attitude Dynamics: A Generalization of the Rodrigues Parameters," *Journal of the Astronautical Sciences*, Vol. 44, No. 1, Jan.-Mar. 1993, pp. 1–19.

[32]Pham, Q.-C., and Slotine, J.-J. E., "Stable Concurrent Synchronization in Dynamic System Networks," *Neural Networks*, Vo. 20, No. 1, 2007, pp. 62-77.

[33]Ploen, S. R., Hadaegh, F. Y., and Scharf, D. P., "Ridgid Body Equations of Motion for Modeling and Control of Spacecraft Formations - Part 1: Absolute Equations of Motion," Proc. of the 2004 American Control Conference, Boston, 2004, pp. 3646–3653.

[34]Strang, G., *Introduction to Applied Mathematics*, Wellesley-Cambridge Press, Wellesey, MA, 1986.

[35]Lim, R. S. and Miller, D. W., "Staged Attitude-Metrology Pointing Control and Parametric Integrated Modeling for Space-Based Optical Systems," Master of Science Thesis, Space Systems Laboratory Report No. 3-06, Dept. of Aeronautics and Astronautics, Massachusetts Inst. of Technology, Massachusetts Institute of Technology, Cambridge, MA, 2006. http://dspace.mit.edu.

[36]Smith, R. S., and Hadaegh, F. Y., "Control of Deep-Space Formation-Flying Spacecraft: Relative Sensing and Switched Information," *Journal of Guidance, Control, and Dynamics*, Vol. 28, No. 1, Jan-Feb 2005, pp. 106–114.